Bioorganic Chemistry 85 (2019) 82–96

Contents lists available at ScienceDirect

Bioorganic Chemistry

journal homepage: www.elsevier.com/locate/bioorg

Biphenyl-3-oxo-1,2,4-triazine linked piperazine derivatives as potential cholinesterase inhibitors with anti-oxidant property to improve the learning and memory

Prabhash Nath Tripathi[a], Pavan Srivastava[a], Piyoosh Sharma[a], Manish Kumar Tripathi[a], Ankit Seth[a], Avanish Tripathi[a], Sachchida Nand Rai[b], Surya Pratap Singh[b], Sushant K. Shrivastava[a,*]

[a] Pharmaceutical Chemistry Research Laboratory, Department of Pharmaceutical Engineering & Technology, Indian Institute of Technology (Banaras Hindu University), Varanasi 221 005 India

[b] Department of Biochemistry, Institute of Science, Banaras Hindu University, Varanasi 221005, India

ARTICLE INFO

Keywords:
Acetylcholinesterase
Butyrylcholinesterase
1,2,4-triazine
Piperazine
PAMPA-BBB
Cognitive dysfunctions
Alzheimer's disease
Donepezil

ABSTRACT

A series of novel piperazine tethered biphenyl-3-oxo-1,2,4-triazine derivatives were designed, and synthesized. Amongst the synthesized analogs, compound **6g** showed significant non-competitive inhibitory potential against acetylcholinesterase (AChE, IC_{50}; 0.2 ± 0.01 μM) compared to standard donepezil (AChE, IC_{50}: 0.1 ± 0.002 μM). Compound **6g** also exhibited significant displacement of propidium iodide from the peripheral anionic site (PAS) of AChE (22.22 ± 1.11%) and showed good CNS permeability in PAMPA-BBB assay ($P_{e(exp)}$, 6.93 ± 0.46). The *in vivo* behavioral studies of compound **6g** indicated significant improvement in cognitive dysfunctions against scopolamine-induced amnesia mouse models. Further, *ex vivo* studies showed a significant AChE inhibition and reversal of the scopolamine-induced oxidative stress by compound **6g**. Moreover, molecular docking and dynamics simulations of compound **6g** showed a consensual binding affinity and active site interactions with the PAS and active catalytic site (CAS) residues of AChE.

1. Introduction

Cognition is a combination of awareness, attention, acquaintance, memory, decision making, and judgments [1]. Cognitive impairment is a pathological condition associated with many neurodegenerative disorders such as Alzheimer's disease (AD), Parkinson's disease (PD), depression, and schizophrenia [2]. The neurotransmitters like acetylcholine (ACh), dopamine, serotonin, glutamate, etc. are responsible for regulating the cognitive symptoms and functionalities. Amongst them, ACh plays a pivotal role in cognitive functionalities as its deficiency in the brain causes memory disorder [3]. ACh is metabolized by acetylcholinesterase (AChE) into choline and acetic acid [4,5]. Hence, the augmentation of ACh level in the brain could be achieved by targeting the AChE through the AChE inhibitors (AChEIs) [6–8]. In the current scenario, there are only three FDA approved AChEIs (donepezil, rivastigmine, and galantamine) available which provide symptomatic cure rather than modifying the disease progression [9]. Therefore, the discovery and development of new drugs for the treatment of AD is required to increase the lifespan of human beings. In the past decade, AChEIs (metrifonate and tesofensine) were identified as promising molecules to treat dementia but withdrawn from the clinical trials due to their toxicity and poor CNS stability [10–12]. Hence, there is an unmet necessity to discover the novel neurotherapeutic agents to diminish the AChE activity and modifying the disease progression.

The oxidative stress is a detrimental factor of memory dysfunctions caused by an imbalance of antioxidant enzymes and overproduction of reactive oxygen species (ROS) such as superoxide anion, hydroxyl radical ($OH^{\bullet}$), and hydrogen peroxide radicals ($H_2O_2^{\bullet}$) [13–16]. These anions and free radicals oxidize various biomolecules and support the progression of the disease. ROS are reported to cause the memory impairment and synaptic plasticity [17,18]. Therefore, AChE inhibitor with promising antioxidant activity could prove itself as a good therapeutic candidate to treat dementia.

1.1. Designing considerations

In this study, the classical bivalent bioisosteric strategy was adopted to design the novel hybrid molecules [19]. The triazine nucleus being

* Corresponding author at: Department of Pharmaceutical Engineering & Technology, Indian Institute of Technology (BHU), Varanasi 221 005, India.
E-mail address: skshrivastava.phe@itbhu.ac.in (S.K. Shrivastava).

https://doi.org/10.1016/j.bioorg.2018.12.017
Received 9 September 2018; Received in revised form 3 December 2018; Accepted 12 December 2018
Available online 15 December 2018
0045-2068/

an attractive moiety was used owing to its binding ability and better inhibition characteristics against several enzymes [20]. Compounds containing 1,2,4-triazine nucleus showed a wide array of applications including the potential AChE inhibitory activities [21–26]. The studies revealed that vicinal biaryl-1,2,4-triazines (**1**) modulate the cholinesterase (ChE) activity through intrinsic antioxidant property [27], whereas 3-Thioalkyl-5,6-biaryl-1,2,4-triazine derivatives (**2**) suppressed the ROS generation and oxidative stress-induced cell death [28]. The 1,2,4-triazine group also displayed a significant role in anchoring the 5,6-biaryl group into the peripheral anionic site (PAS) of AChE through hydrophobic interactions [29]. Additionally, the molecule containing 5,6-biaryl-3-oxo-1,2,4-triazine group were reported to devoid of gastric or cardiac toxicity [30,31]. Therefore, the 5,6-biaryl-3-oxo-1,2,4-triazine was chosen as a core scaffold and tethered with other pharmacophoric functionalities.

Donepezil (**3**) is an FDA approved drug used for the treatment of dementia having benzyl piperidine nucleus, which is oriented towards the catalytic active site (CAS) of AChE [32–34]. The piperazine moiety was chosen in place of piperidine ring owing to the bioisosteric nature. Though piperazine ring possesses lower AChE affinity [35], but several compounds comprising this nucleus have been reported for nootropic effect with substantial neuroprotective activity [36–38].

Therefore, molecular hybrids consisted of the 5,6-biphenyl-3-oxo-1,2,4-triazine nucleus and substituted piperazines were connected using the different lengths of alkyl linkers and evaluated for their potential ChE inhibition and antioxidant properties (Fig. 1). In the present work, biphenyl-3-oxo-1,2,4-triazine linked piperazine analogs were synthesized and evaluated for ChE inhibition, propidium iodide displacement, BBB permeability, and neuroblastoma cell line assay. The propitious compound was further subjected to *in vivo* behavioral studies by scopolamine-induced mouse models. The *ex vivo* studies and biochemical estimation of the oxidative stress biomarkers were also affirmed their AChE inhibitory and antioxidant potential, respectively. Finally, the interactions and binding modes of the compound **6g** on active site of AChE were assessed by *in silico* molecular docking and dynamic simulations studies.

2. Results and discussion

2.1. Chemistry

The target compounds (**5a-g, 6a-g, 7a-g,** and **8a-g**) were synthesized according to Scheme 1. Initially, 5,6-Biphenyl-3-oxo-1,2,4-triazine (**4**) was synthesized by refluxing 1,2-diphenylethandione with semicarbazide hydrochloride in the presence of glacial acetic acid [31]. Compound **4** was further reacted with different bromochloroalkanes in the presence of potassium hydroxide and *N, N*-dimethylformamide (DMF) to afford the key intermediates (**5, 6, 7** and **8**). In ^{1}H NMR spectra, the disappearance of (-N**H**) proton peak of compound **4**, and the appearances of triplet signal of two protons of (*N*-C**H**$_2$) between 4.53 and 4.29 ppm (J = 7.0 Hz) and multiplates of ten protons of biphenyl group at 7.51–7.28 ppm. ^{13}C NMR spectral assignment was based on the distinctive carbon peaks of all the synthesized derivatives. ^{13}C NMR spectra of compounds (**5, 6, 7,** and **8**) displayed the characteristic signals of -N-**C**H$_2$ and -**C**H$_2$-Cl at 53.0–49.8 ppm, and 44.7–41.0 ppm, respectively. The signal of carbonyl (triazinone, > C = O) of 1,2,4-triazine-3-oxo nucleus appeared at 166.5–166.2 ppm. The target compounds (**5a-g**, **6a-g**, **7a-g**, and **8a-g**) were synthesized by refluxing the intermediates (**5, 6, 7** and **8**) with various piperazines in the presence of potassium carbonate, potassium iodide, and acetonitrile. The synthesized compounds were preliminarily identified by positive Dragendroff test on TLC (Thin Layer Chromatography) [39,40] and further purified by column chromatography to afford the pure compounds (60–84% yield). ^{1}H NMR spectra of compounds (**5a-g, 6a-g, 7a-g,** and **8a-g)** showed the presence of methylene protons (C**H**$_2$-N) and absence of single -N**H** proton of piperazine moieties. The compounds having 2-pyridyl (**5d, 6d, 7d,** and **8d**) moiety exhibited the signals in the range of 8.31–6.60 ppm. The compounds (**5e, 6e, 7e,** and **8e**) bearing 4-methoxy substituent showed a diagnostic singlet peak of three protons between 3.73 and 3.62 ppm. The compounds (**5f, 6f, 7f,** and **8f**) having biphenyl methyl (-C**H**) group exhibited a distinctive singlet peak of one proton approximately at ~4.12 ppm. Compounds (**5g, 6g, 7g,** and **8g**) displayed the characteristic signals of two protons (*N*-C**H**$_2$-phenyl) between 3.45 and 3.19 ppm. In the ^{13}C NMR spectra, the compounds (**5e, 6e, 7e,** and **8e**) having 4-methoxyphenyl piperazine displayed the signals of methoxy (-O**C**H$_3$), and methoxy attached carbon between 57.7 and 55.6, 153.7–152.9 ppm, respectively. The synthesized derivatives (**5f, 6f, 7f,** and **8f**) with biphenyl methyl (-**C**H) group exhibited a diagnostics signals at around ~76.3 ppm. The distinctive piperazine-**C**H$_2$-phenyl signals of the compounds (**5g, 6g, 7g,** and **8g**) appeared at 63.2–62.9 ppm. The purity of all the synthesized compounds was determined by elemental analyses, and their results were found within ± 0.4% range of the theoretical values.

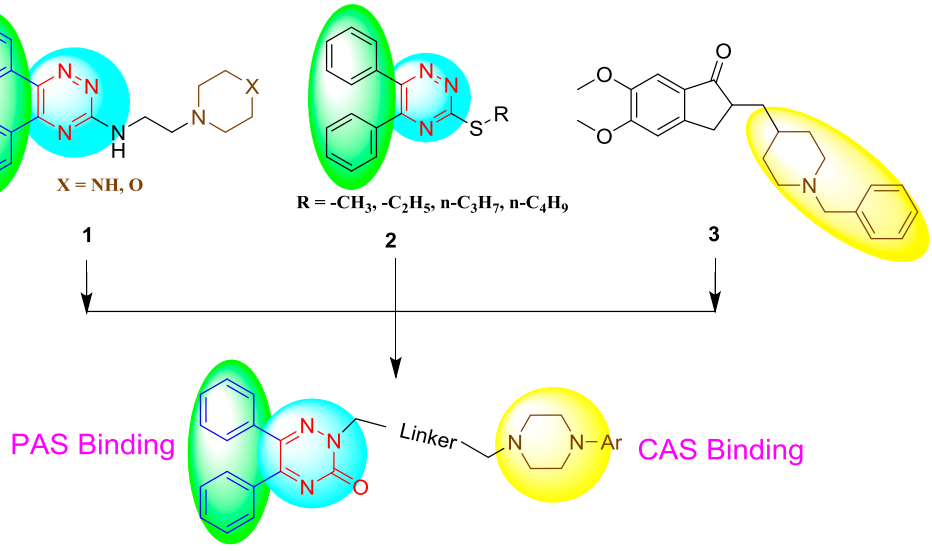

Fig. 1. The designed compounds.

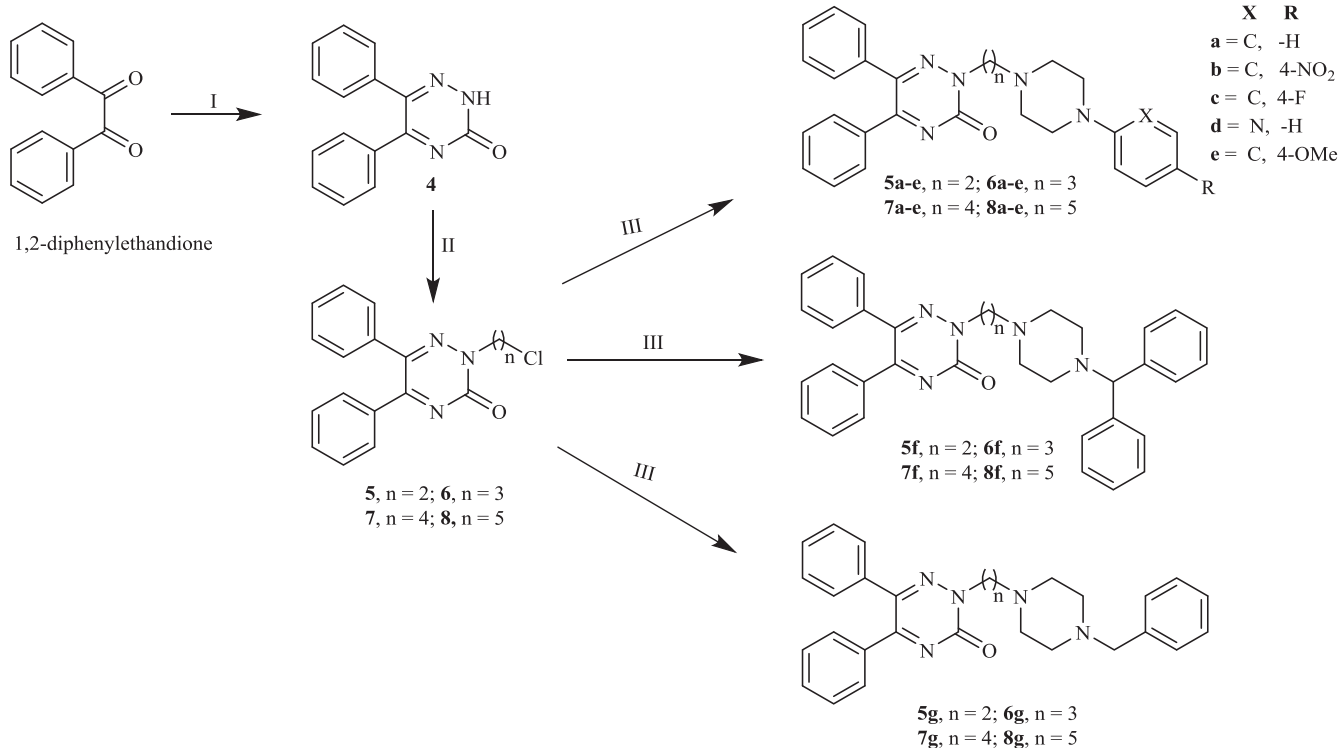

Scheme 1. Reagents and conditions: (I) semicarbazide hydrochloride, glacial acetic acid, reflux; (II) potassium hydroxide, $Br(CH_2)_nCl$ (n = 2, 3, 4, and 5), DMF, room temperature, 1 h; (III) substituted piperazines, anhydrous potassium carbonate, potassium iodide, acetonitrile, reflux, 13 h.

2.2. Pharmacology

2.2.1. In vitro cholinesterase inhibition assay

All the synthesized compounds (**5a-g, 6a-g, 7a-g,** and **8a-g**) and standard donepezil were screened for ChE inhibition activity using Ellman's method (Table 1).

The enzyme inhibition activity of all the synthesized compounds was analyzed by concerning the variations of alkyl linkers (n = 2, 3, 4, 5) and substituents attached to the terminal end of piperazine moiety.

Variation of carbon chain linkers

The methylene linkers (n = 2–5) formed a bridge between 5,6-biphenyl-3-oxo-1,2,4-triazine core group and various substituents of the piperazine nucleus and resulted compounds were evaluated for ChE inhibition. The results indicated that lengthening of carbon chain increased the lipophilic characteristics and hindered the freedom of C-C bond rotation [41,42]. Overall, three carbon chain (n = 3) was found to be optimal linker for AChE inhibition.

The compounds (**5f, 6f, 7f,** and **8f**) containing benzhydryl piperazine group at the terminal end not showed any significant inhibitory activity with various linkers. The literature also revealed that very high hydrophobicity hindered the binding of compounds at the active site of AChE [43].

Variation of terminal piperazine functionalities

The compounds (**6a-g**) bearing propyl (n = 3) linker showed a promising AChE inhibitory activity. Thereby, our discussion is more focused on compounds (**6a-g**). The compound **6a** consisting of phenylpiperazine moiety displayed an acceptable AChE inhibitory activity (IC_{50} = 0.6 ± 0.05 μM). The electron-withdrawing (nitro, **6b**; and fluoro, **6c**) and electron donating (methoxy, **6e**) substituents at *para* position of phenylpiperazine ring increased the AChE inhibition (**6b**, IC_{50}; 0.5 ± 0.02 μM; **6c**, IC_{50}; 0.4 ± 0.03 μM; **6e**, IC_{50}; 0.3 ± 0.03 μM). Interestingly, compound **6e** having 4-methoxyphenyl group showed better AChE inhibition compared to compound **6b** and **6c**. The improvement in AChE inhibitory potential might be because of non-polar characteristics of OCH_3 group which interacted with the hydrophobic pocket of AChE [44]. In the comparison amongst compounds bearing different electron withdrawing substituents, compound **6c** having a fluoro substituent showed slightly better inhibitory potential against the AChE compared to compound **6b** with a nitro substituent. The reason for better inhibitory activity could be the high electronegativity of fluorine atom that modulates the lipophilicity of the molecule [45]. The compound **6d** with 2-pyridyl piperazine displayed a lower AChE inhibition (IC_{50}; 1.1 ± 0.09 μM) compared to compounds **6a, 6b, 6c, 6e,** and **6g**.

Amongst all the tested derivatives, compound **6g** bearing three carbon atoms linked with benzylpiperazine terminal group showed potent inhibition against the AChE (IC_{50} = 0.2 ± 0.01 μM). The AChE inhibitory activity of compound **6g** also comparable with standard donepezil (IC_{50} = 0.01 ± 0.002 μM) because of the benzyl group engaged at the bottom of the enzyme gorge and better interacted with CAS residues of AChE [46].

All the synthesized compounds were further tested for their BChE inhibitory effect but failed to exhibit any significant activity. The probable reason for this might be the wider BChE gorge than AChE owing to the replacement of two aromatic amino acids by the smaller aliphatic amino acids [47].

2.2.2. Enzyme kinetics study

The synthesized compounds (**5a-g, 6a-e, 6g, 7a-c, 7e, 7g** and **8a-b, 8g**) were subjected to enzyme kinetics studies, and the results are reported in Table 1. The substrate-dependent enzyme kinetics elucidated the mode of enzyme inhibition for the most active compound **6g** using the Lineweaver-Burk reciprocal $1/V_{max}$ Vs. 1/S plot, which suggested the non-competitive type of enzyme inhibition of AChE (Ki = 0.2 ± 0.01 μM) (Fig. 2).

2.2.3. Propidium iodide displacement assay

Propidium iodide assay was used to determine the displacement of propidium iodide (a selective PAS-AChE inhibitor) from the propidium iodide-AChE enzyme complex [48]. The binding of compounds at PAS

Table 1
The results of ChE inhibition assay, selectivity index, and enzyme kinetics study.

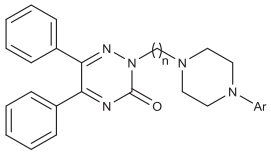

Comp. Code	n	Ar	AChE IC_{50} (μM) ± SD	BChE IC_{50} (μM) ± SD	[a]SI ratio	AChE Ki (μM) ± SD	Types of Inhibition (AChE)
5a	2	$-C_6H_5$	1.2 ± 0.08*	> 50	–	0.9 ± 0.08	nc
5b	2	$4\text{-}NO_2C_6H_5$-	0.6 ± 0.04*	11.2 ± 0.96	20	0.5 ± 0.04	nc
5c	2	$4\text{-}FC_6H_5$-	0.9 ± 0.06*	> 50	–	0.7 ± 0.07	nc
5d	2	$-C_5H_4N$	1.8 ± 0.11*	19.5 ± 1.12	11	1.4 ± 0.1	nc
5e	2	$4\text{-}OCH_3C_6H_5$-	0.6 ± 0.04*	> 50	–	0.5 ± 0.04	nc
5f	2	$-CH(C_6H_5)_2$	0.5 ± 0.04*	> 50	–	0.4 ± 0.03	nc
5g	2	$-CH_2\text{-}C_6H_5$	0.5 ± 0.04*	> 50	–	0.3 ± 0.03	nc
6a	3	$-C_6H_5$	0.6 ± 0.05*	> 50	–	0.5 ± 0.05	nc
6b	3	$4\text{-}NO_2C_6H_5$-	0.5 ± 0.02*	> 50	–	0.4 ± 0.03	nc
6c	3	$4\text{-}FC_6H_5$-	0.4 ± 0.03*	5.2 ± 0.19	15	0.3 ± 0.02	nc
6d	3	$-C_5H_4N$	1.1 ± 0.09*	> 50	–	0.9 ± 0.09	nc
6e	3	$4\text{-}OCH_3C_6H_5$-	0.3 ± 0.03*	> 50	–	0.3 ± 0.02	nc
6f	3	$-CH(C_6H_5)_2$	> 5*	–	–	nt	–
6g	3	$-CH_2\text{-}C_6H_5$	0.2 ± 0.01 ns	4.6 ± 0.19	23	0.2 ± 0.01	nc
7a	4	$-C_6H_5$	1.9 ± 0.12*	> 50	–	1.5 ± 0.9	nc
7b	4	$4\text{-}NO_2C_6H_5$-	0.6 ± 0.04*	> 50	–	0.5 ± 0.04	nc
7c	4	$4\text{-}FC_6H_5$-	1.4 ± 0.13*	23.3 ± 2.19	17	1.1 ± 0.99	nc
7d	4	$-C_5H_4N$	> 5*	> 50	–	nt	–
7e	4	$4\text{-}OCH_3C_6H_5$-	0.5 ± 0.03*	> 50	–	0.4 ± 0.03	nc
7f	4	$-CH(C_6H_5)_2$	> 5*	–	–	nt	–
7g	4	$-CH_2\text{-}C_6H_5$	0.6 ± 0.05*	8.6 ± 0.54	13	0.5 ± 0.05	nc
8a	5	$-C_6H_5$	2.2 ± 0.19*	> 50	–	1.8 ± 0.14	nc
8b	5	$4\text{-}NO_2C_6H_5$-	1.9 ± 0.15*	9.3 ± 0.84	5	1.6 ± 0.13	nc
8c	5	$4\text{-}FC_6H_5$-	> 5*	> 50	–	nt	–
8d	5	$-C_5H_4N$	> 5*	> 50	–	nt	–
8e	5	$4\text{-}OCH_3C_6H_5$-	> 5*	> 50	–	nt	–
8f	5	$-CH(C_6H_5)_2$	> 5*	> 50	–	nt	–
8g	5	$-CH_2\text{-}C_6H_5$	1.7 ± 0.16*	> 50	–	1.4 ± 0.97	nc
donepezil	–	–	0.1 ± 0.01	4.1 ± 0.28	48	nt	–

Values are presented as mean ± S.D (n = 3) and analyzed by one-way ANOVA followed by Dunnett's test.
* $p < 0.05$ compared to standard donepezil, ns = Non-significant.
[a] Selective index ratio = (BChE IC_{50})/(AChE IC_{50}). nc = non-competitive; nt = not tested.

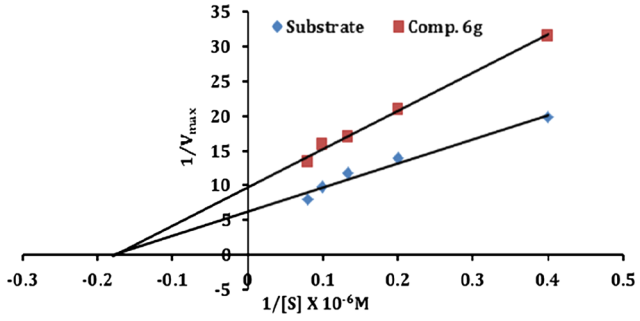

Fig. 2. Lineweaver-Burk plot showing non-competitive inhibition of compound **6g.**

of AChE leads to diminished fluorescence intensity with the displacement of propidium iodide. All the tested derivatives showed substantial displacement of propidium iodide (17.45–22.22%) except compounds **6b** and **6d.** The results also indicated that compound **6g** could efficiently bound to the PAS site of AChE (Table 2).

2.2.4. Parallel artificial membrane permeation assay (PAMPA-BBB)

The selected compounds (**6a-e,** and **6g**) were screened through PAMPA-BBB assay [49]. Among of all the derivatives, standard donepezil and compound **6g** showed P_e more than (4.3926×10^{-6} cm/s) indicated their high BBB permeation (Table 2).

Table 2
Propidium iodide displacement and Permeability analysis using PAMPA-BBB assay.

Comp.	Propidium Iodide Displacement (%)[a]	PAMPA-BBB permeability $P_{e(exp)}$ (10^{-6} cm s^{-1})	PAMPA-BBB Prediction (CNS +[b], CNS-[c], CNS ±[d])
6a	21.45 ± 1.72*	3.29 ± 0.27*	CNS ±
6b	12.54 ± 0.87*	4.63 ± 0.32*	CNS +
6c	17.84 ± 1.38 ns	4.21 ± 0.21*	CNS ±
6d	13.15 ± 0.79*	4.48 ± 0.32*	CNS +
6e	17.45 ± 0.80 ns	4.85 ± 0.29*	CNS +
6g	22.22 ± 1.11*	6.93 ± 0.46ns	CNS +
Donepezil	17.33 ± 1.38	7.28 ± 0.43	CNS +

Values are presented as the mean ± S.D (n = 3) and analyzed by one-way ANOVA followed by Dunnett's test.
* $p < 0.05$ compared to standard donepezil, ns = No significant.
[a] Propidium iodide displacement assay was performed on eeAChE.
[b] 'CNS + ' (prediction of high BBB permeation); P_e (10^{-6} cm s^{-1}) > 4.3926.
[c] 'CNS-' (prediction of low BBB permeation); P_e (10^{-6} cm s^{-1}) < 1.7766.
[d] 'CNS ± ' (prediction of uncertain BBB permeation); P_e (10^{-6} cm s^{-1}) 4.3926 to 1.7766.

2.2.5. Neurotoxicity assay

The 3-(4,5-Dimethylthiazol-2-yl)-2,5-diphenyl tetrazolium bromide (MTT) colorimetric assay was used to determine the neurotoxicity against SH-SY5Y neuroblastoma cell lines [50]. The compound **6g** and

Table 3
In vitro neurotoxicity on SH-SY5Y cell lines.

Comp.	Mean ± SD (IC_{50})
6g	83.8 ± 6.87
Donepezil	86.9 ± 7.42

Values are presented as the mean ± S.D (n = 3).

donepezil showed the IC_{50}; 83.78 ± 6.87 μM and IC_{50}; 86.9 ± 7.42 μM, respectively (Table 3).

2.2.6. *In vivo behavioral studies*

Owing to considerable *in vitro* anti-ChE activity, propidium iodide displacement activity, and predicted high CNS permeability, the potential compound **6g** was further evaluated for *in vivo* learning and memory through scopolamine-induced mouse models [18].

2.2.6.1. Acute oral toxicity study. The acute toxicity of compound **6g** was determined as per the OECD 423 guidelines on healthy Swiss albino mice (25–30 gm). All the mice were observed for mortality up to 14 days post-treatment period. The dose of 500 mg/kg, p.o. of compound **6g** was well tolerated and suggested a significant margin of safety [51].

2.2.6.2. Y-maze test in mice. Y-maze test is a standard neurobehavioral experiment to evaluate the hippocampal-dependent short-term memory in the rodents [52]. The compound **6g** treated groups showed a dose-dependent increase in spontaneous alteration rate. Interestingly, compound **6g** (10 mg/kg) attenuated the dysfunctions of alteration rate with a non-significant difference to the donepezil-treated group (5 mg/kg). Further, spontaneous alteration rate significantly declined in the scopolamine-treated group suggested the induction of memory impairment (Fig. 3A). The total numbers of arm entries showed a non-significant difference amongst all groups, indicated that scopolamine-treated group did not affect the locomotive behavior in mice (Fig. 3B). The results suggested that compound **6g** reversed the scopolamine-induced cognitive dysfunctions in mice.

2.2.6.3. Passive avoidance test. The transfer latency time (TLT) was calculated to evaluate the memory impairment in mice. There was no significant alteration observed in TLT during acquisition test compared to retention test of the scopolamine-treated group. Whereas, the compound **6g**-treated group significantly increased the TLT in a dose-dependent manner during the retention test. The effect of compound **6g** at the dose of 10 mg/kg was comparable with the donepezil-treated group (5 mg/kg) (Fig. 4).

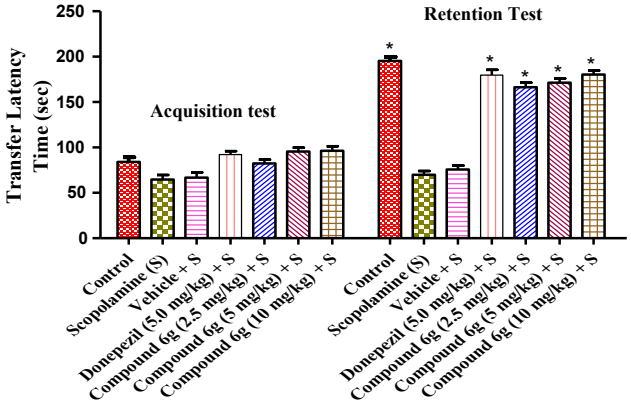

Fig. 4. Effect of compound **6g** in the passive avoidance test. Bars display values as mean ± SD (n = 6) and analyzed by one-way ANOVA followed by Tukey's Test *p < 0.05 compared to the respective groups of acquisition test.

2.2.7. *Neurochemical estimation of AChE*

The ex vivo study was conducted to estimate the AChE in mice brain homogenates using Ellman colorimetric assay. Compound **6g** (10 mg/kg)-treated group showed a low rate of hydrolysis compared to scopolamine-treated group and also reflected that compound **6g** inhibited the AChE and penetrated the BBB (Fig. 5A).

2.2.8. *Biochemical estimation of the oxidative stress factors*

Oxidative stress is an important damaging factor for neurodegenerative disorders [53]. The compound **6g** was investigated for the neuroprotective activity to address the oxidative stress in animals with cognitive dysfunctions. The malondialdehyde (MDA), glutathione (GSH), superoxide dismutase (SOD), catalase enzyme, and nitrite (NO_2^-) levels were quantitatively analyzed using mice brain homogenates.

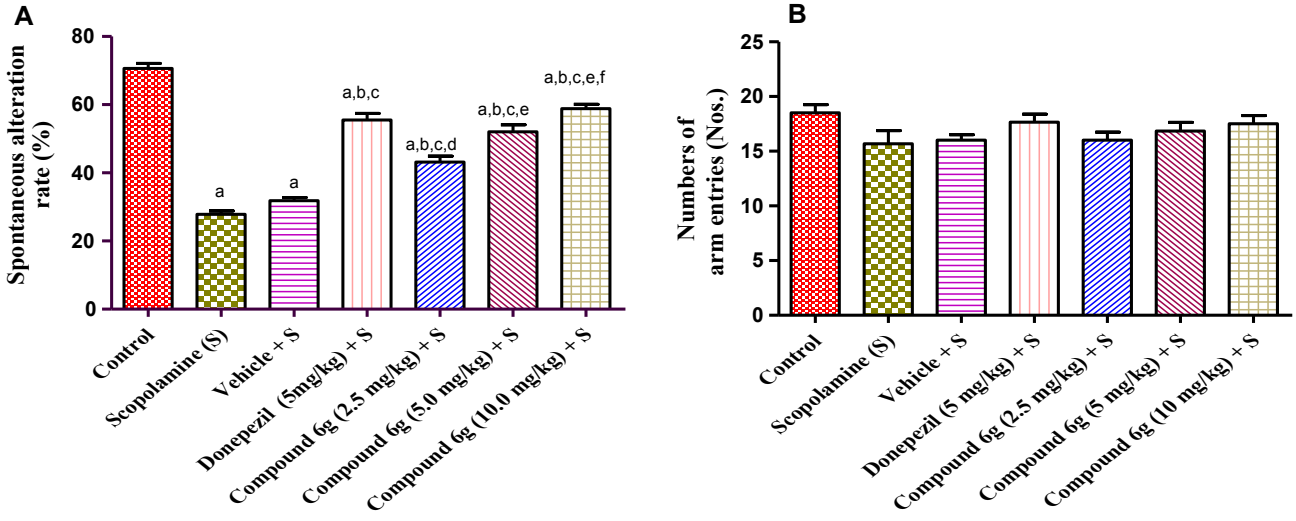

Fig. 3. Effect of compound **6g** (2.5, 5 and 10 mg/kg, p.o.) in the y-maze test. (A) Spontaneous alterations rate; (B) Number of arm entries; Bars display values as mean ± SD (n = 6) and analyzed by one-way ANOVA followed by Tukey's test; [a]p < 0.05 as compared to control; [b]p < 0.05 as compared to scopolamine; [c]p < 0.05 as compared to vehicle; [d]p < 0.05 as compared to donepezil; [e]p < 0.05 as compared to compound **6g** at dose of 2.5 mg/kg; [f]p < 0.05 as compared to compound **6g** at dose of 5 mg/kg.

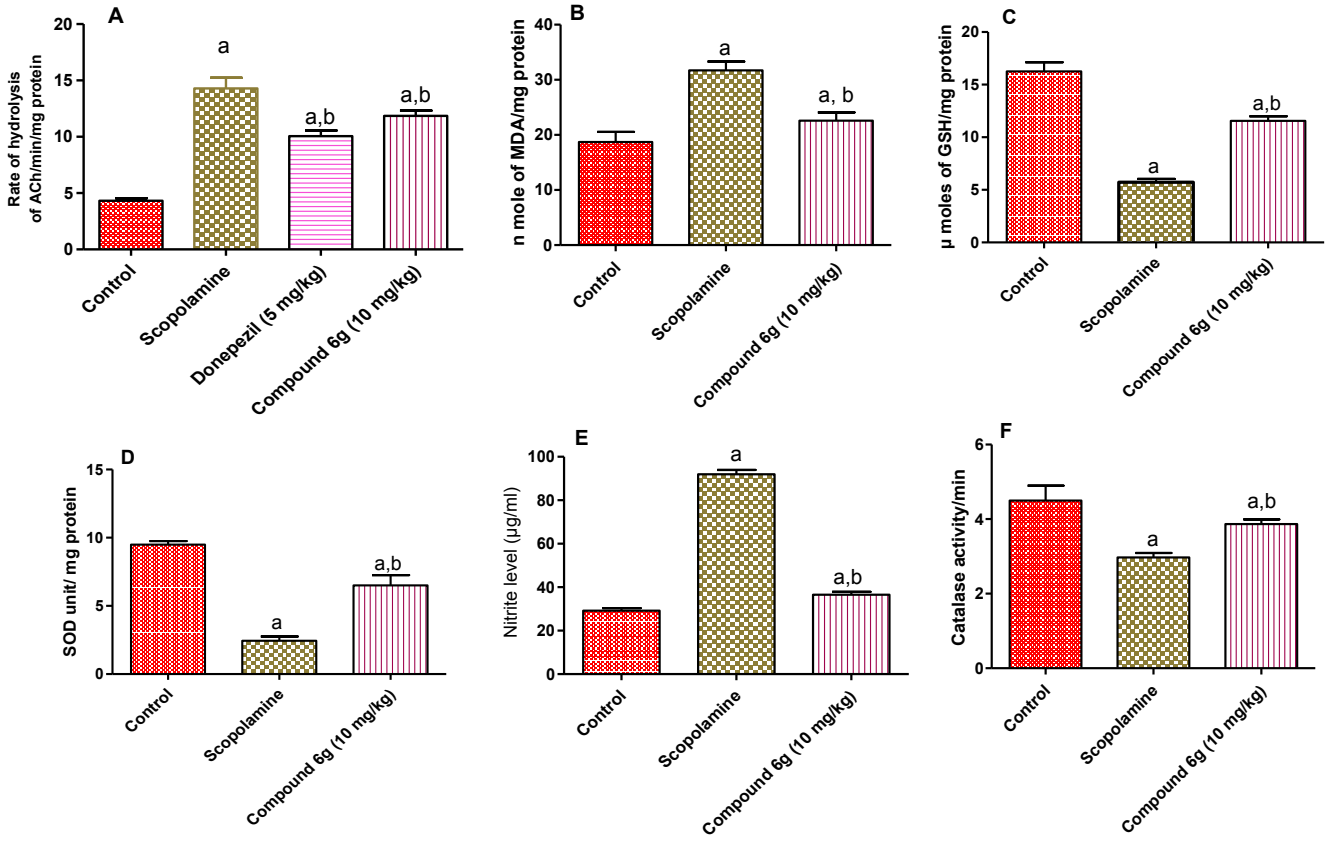

Fig. 5. The results of *ex vivo* and biochemical analysis (A) AChE activity; (B) Malonaldehyde (MDA); (C) Reduced glutathione (GSH); (D) Superoxide dismutase (SOD); (E) Nitrite concentration and; (F) Catalase levels on scopolamine-induced of the cholinergic deficit and oxidative stress. The values presented as mean ± SD (n = 3) and analyzed by one-way ANOVA, followed by Tukey's test. $^{a}p < 0.05$ as compared to control; $^{b}p < 0.05$ as compared to scopolamine.

2.2.8.1. 2-Thiobarbituric acid reactive substances (TBRAS). The TBARS assay was used to analyze the malondialdehyde (MDA) levels in the brain homogenates. The compound **6g** (10 mg/kg) treated group exhibited a significant reduction in malondialdehyde (MDA) concentration compared to scopolamine-treated group (Fig. 5B).

2.2.8.2. Reduced glutathione estimation. Ellman's method was used for the estimation of reduced glutathione (GSH). Glutathione is a natural antioxidant tri-peptide thiol agent (L-glutamyl-L-cysteinylglycine) neutralizes the generation of ROS during the cellular oxidative stress. The results revealed that compound **6g** (10 mg/kg) treated group showed a significantly higher GSH level compared to scopolamine-treated group (Fig. 5C).

2.2.8.3. Superoxide dismutase (SOD) assay. The superoxide dismutase estimation was based on the production of superoxide (O_2^-) radical. SOD generally consumes the O_2^- radicals of the biological system. The SOD level significantly raised by the compound **6g** (10 mg/kg) compared to scopolamine-treated group. (Fig. 5D).

2.2.8.4. Nitrite (NO_2^-) assay. The Griess reagent was used to analyze the nitrite ion. The results showed that compound **6g** (10 mg/kg) treated group significantly reduced the nitrite concentration in the brain compared to scopolamine-treated group (Fig. 5E).

2.2.8.5. Catalase assay. Catalase assay signifies the decomposition of hydrogen peroxide (H_2O_2) into water (H_2O) by the catalase. Interestingly, Compound **6g** (10 mg/kg) significantly averted the loss of catalase activity compared to scopolamine-treated group (Fig. 5F).

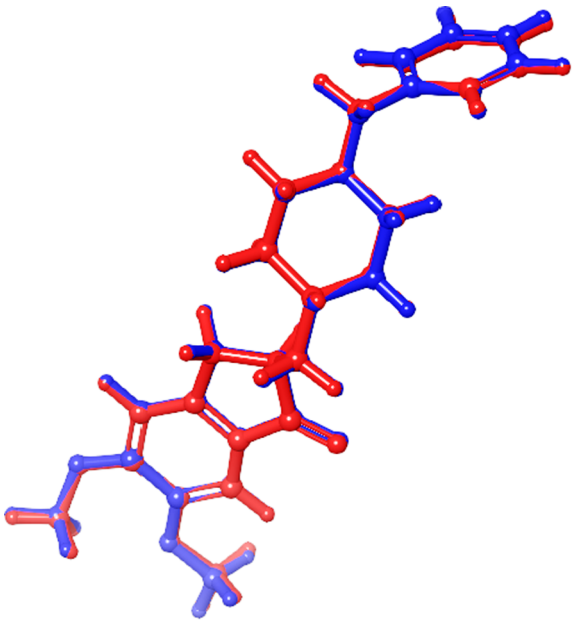

Fig. 6. Superposition of re-docked (red) and co-crystallized (blue) poses of donepezil on AChE (PDB Code: 1EVE).

2.3. Computational studies

2.3.1. In silico molecular docking studies

Molecular docking studies were performed to explore the binding affinity and binding pattern of compound **6g** in the active sites of AChE

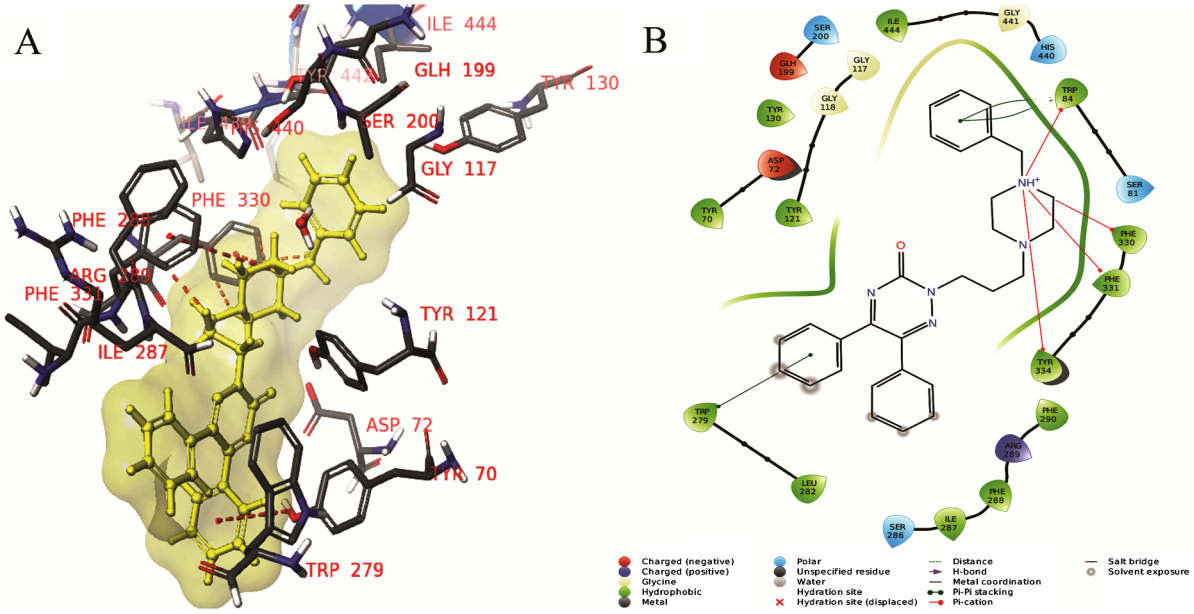

Fig. 7. The docking of compound **6g** on AChE enzyme. (A) 3D interaction image showing compound **6g** in the ligand binding surface (yellow color) interacting with active site residues of AChE; (B) 2D image showing active site interactions.

Table 4
In silico docking interaction analysis of compound **6g** and donepezil on AChE.

Comp.	Interacting residues[#]					
	CAS	PAS	Anionic subsite	Acyl binding pocket	Oxyanion hole	Other interacting residues
6g	Ser200[a], His440[a]	Trp279[b], Tyr334[e], Tyr70[c], Tyr121[c], Asp72[d]	Glu199[d], Trp84[b,e], Phe330[c]	Phe288[c], Phe290[c], Phe331[c]	Gly117[f], Gly118[f]	Ser81[a], Tyr130[c], Leu282[c], Ser286[a], Ile287[c], Arg289[d], Gly441[f], Ile444[c]
Donepezil	Ser200[a], His440[a]	Trp279[b], Tyr334[e], Tyr70[c], Tyr121[c], Asp72[d]	Glu199[d], Trp84[b,e] Phe330[c]	Phe288[c], Phe290[c], Phe331[c]	Gly117[f], Gly118[f]	Tyr130[c], Leu282[c], Ser286[a], Ile287[c], Arg289[d], Gly441[f], Ile444[c]

[#] All the interacting residues are within the 4 Å distance with the ligand;
[a] polar interaction;
[b] π-π stacking interaction;
[c] hydrophobic interaction;
[d] charged interaction;
[e] π-cation interaction;
[f] glycine interaction.

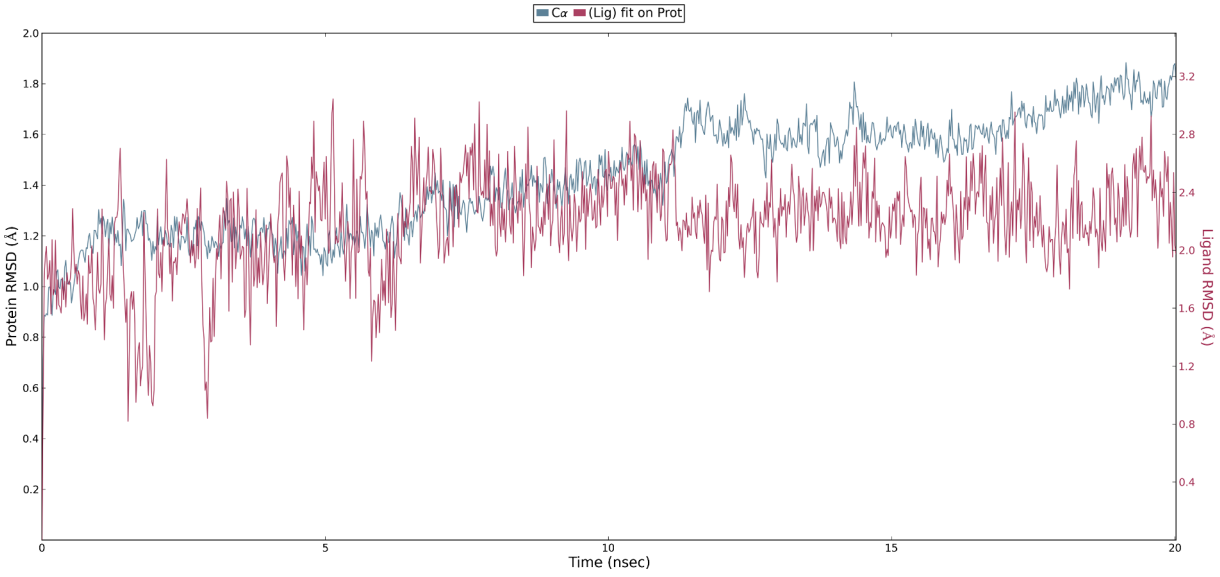

Fig. 8. RMSD graph of the compound **6g**-AChE complex for the period of 20 ns dynamics simulations.

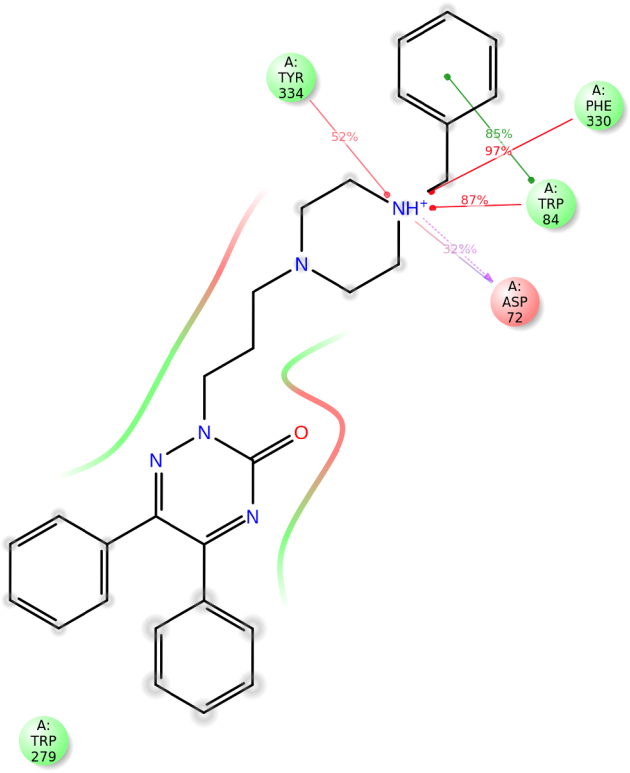

Fig. 9. Graphical representation of compound **6g** showing interacting residues for the simulations of 20 nsec.

(PDB Code: 1EVE) using Glide module of Schrödinger Maestro 2018–1. Initially, the prepared enzyme grid and docking protocols were validated by extracting and re-docking of co-crystallized ligand (donepezil). Furthermore, the poses of re-docked and co-crystallized ligands were compared using superposition tool, and the RMSD value was observed within the range of 3 Å (Fig. 6).

The docked scores of the compound **6g** and donepezil were found to be −14.1 and −13.6 kcal/mole, respectively. The ligand interaction diagram of donepezil and AChE showed their strong binding affinity with the active site residues of AChE. The benzylpiperidine nucleus of donepezil interacted via π–cation interactions at the anionic subsite (Trp84, Phe330) and PAS (Tyr334), and observed to fit completely into the CAS of AChE. Some polar interactions of compound **6g** were also observed with His440 and Ser200, whereas the indanone nucleus of donepezil interacted effectively to the Trp279 of PAS via π–π stacking (Suppl. Fig. S1). The active compound **6g** and donepezil were superimposed and showed a similar type of interaction at the active pocket of AChE (Suppl. Fig. S2). Docking analysis of compound **6g** revealed that benzylpiperazine moiety interacted with His440 and Ser200 through polar interactions in the CAS. Interestingly, the most significant interaction found with the Trp84 of anionic subsite of AChE where the compound **6g** exhibited the π-π stacking and cation-π interaction with the Trp84. Also, the quaternary nitrogen showed cation-π interaction with the Phe330, Phe331, and Phe334 (Fig. 7A and 7B). The biaryl nucleus of compound **6g** further exhibited π-π stacking interactions with amino acids Trp279 at the PAS of AChE (Table 4).

2.3.2. *Molecular dynamics (MD) simulations*

The stability of docked binding pose of the compound 6g-AChE complex was analyzed by molecular dynamics simulation analysis using Desmond (DE Shaw Research). The molecular dynamics simulations analyzed the stability of the docked complex in a flexible protein environment in the presence of virtual water molecules. The root means square deviations (RMSD) values were calculated for the docked complexes and compared with reference protein backbone structures which were within the range (Fig. 8). Root mean square fluctuations (RMSF) values also indicated stable trajectories of the ligand and protein residues throughout the simulation analysis (Suppl. Fig. S3).

The detailed interaction analysis was carried out using the protein-ligand histogram (Suppl. Fig. S4), graphical (Fig. 9), and time-line representation (Fig. 10). The percentage of interactions of the protein residues with compound **6g** were identified using protein-ligand contacts. The PAS region of Tyr334 formed π-cation interaction with compound **6g** for 52% time-scale. The nitrogen atom (N-4) of the piperazine ring of compound **6g** displayed a hydrogen bonding with the Asp72 residue. The phenyl ring of benzylpiperazine nucleus formed π-π stacking interaction with the Trp84 at anionic subsite on 85% time-scale. The piperazine -NH also showed π-cation interactions with the Trp84 and Phe330 at 87% and 97% time-scales, respectively.

In a nutshell, the biaryl structure of compound **6g** showed the

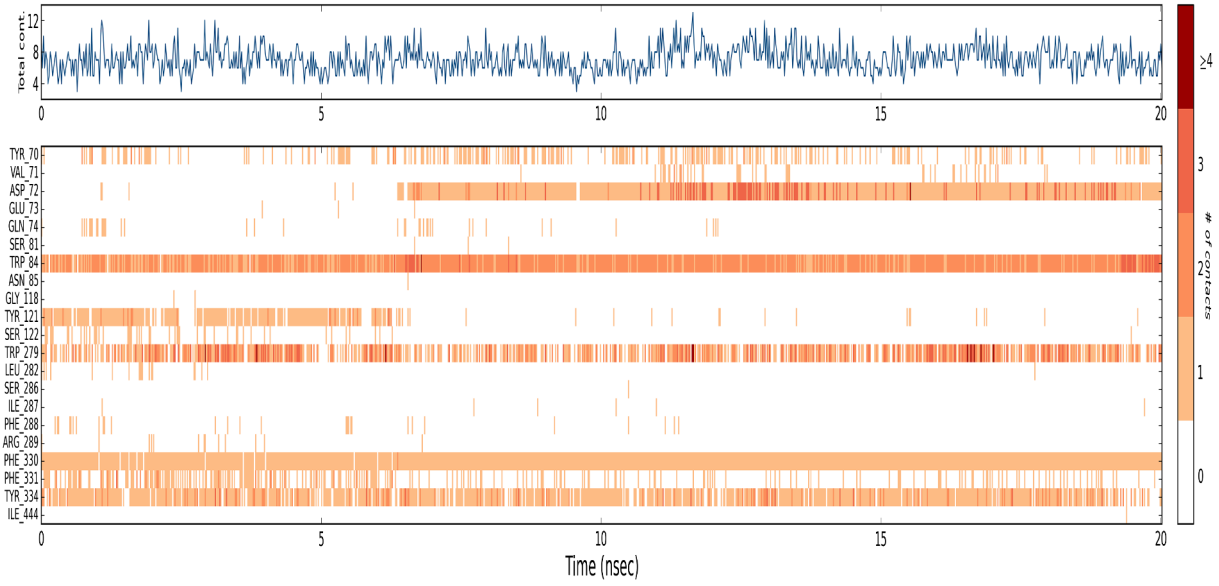

Fig. 10. A timeline representation of the compound **6g**-AChE.

Table 5
QikProp analysis of compound **6g.**

Compound	Mol_MW[a]	Donor HB[b]	Acceptor HB[c]	SASA[d]	QplogBB[e]	Qplog Po/w[f]	Qpp MDCK[g]	Qplog Khsa[h]
Donepezil	393.61	1	7.1	759.67	0.14	4.25	595.28	0.69
6g	465.59	0	7	827.23	0.27	4.99	113.28	0.76

[a] Mol_MW- Molecular weight of the molecule (130 to 725).
[b] Donor HB- number of hydrogen bonds (0.0 to 6.0).
[c] Acceptor HB- number of hydrogen bonds (2.0 to 20.0).
[d] SASA- total solvent accessible surface area (SASA) in square angstroms using a probe with a 1.4 Å radius (300 to1000).
[e] QPlogBB- predicted brain/blood partition coefficient (-3.0 to 1.2).
[f] QPlogPo/w- this gives the predicted octanol/water partition coefficient (-2.0 to 6.5).
[g] QPPMDCK- predicted MDCK cell permeability in nm/s using the Affix scale (< 25 is considered poor and > 500 is considered excellent).
[h] QPLog Khsa- prediction of binding to human serum albumin (-1.5 to 1.5).

hydrophobic interaction with Trp279, the phenyl group of benzylpiperazine moiety and the nitrogen atom of piperazine exhibited π-π stacking interaction (85% time-scale) and cation-π interaction (87% time-scale) with Trp84 of anionic subsite of the AChE, respectively. The quaternary nitrogen of piperazine also depicted π-cation interaction with Tyr334 (52% time-scale) and Phe330 (97%).

2.3.3. Drug-likeliness by QikProp module

Compound **6g** was evaluated for drug-likeliness characteristics using the QikProp module of Schrödinger, and the result was found comparable with standard donepezil Table 5. The predicted QPlogKhsa values affirm their strong binding with plasma protein. The outcome of Lipinski's rule of five (mol_MW < 500, QPlog Po/w < 5, donorHB 0–6.0, accptHB 2.0–20), along with the other predicted parameters (SASA 300–1000, QPlogBB −3.0 to 1.2, QPlogPo/w −2.0 to 6.5) reflected that the compound **6g** elicited "drug-like" characteristics.

3. Conclusion

A series of novel hybrids were designed and synthesized by combining the piperazine nucleus with vicinal biphenyl-3-oxo-1,2,4-triazine through varied alkyl linkers. Amongst all the synthesized compounds, **6a-g** with propyl (n = 3) linker displayed the better *in vitro* AChE inhibitory potential. The benzylpiperazine tail containing compound **6g** revealed the most significant inhibitory potency (AChE, IC_{50} = 0.2 ± 0.01 μM) as standard donepezil (AChE, IC_{50} = 0.1 ± 0.002 μM) with non-competitive type of inhibition. Therefore, the AChE inhibitory activity was more accountable with alkyl linkers and piperazine substituents. Further, PI displacement assay showed significant displacement of propidium iodide with compound **6g** (22.22 ± 1.11%) from PAS of AChE along with high BBB permeability. Additionally, compound **6g** exhibited the IC_{50}; 83.8 ± 6.87 μM against the neuroblastoma cell line as determined by MTT assay. *In vivo* behavioral studies in mice models revealed that compound **6g** (10 mg/kg) significantly reversed the scopolamine-induced cognitive impairment comparable to that of standard donepezil (5 mg/kg). The *ex vivo* and biochemical analysis of oxidative stress biomarkers indicated significant AChE inhibition and reversed the scopolamine-induced oxidative stress by compound **6g**. Furthermore, the molecular docking and dynamics simulations studies substantiated our findings that compound **6g** consensually interacted with PAS and CAS residues of AChE. Overall, the novel derivatives of biphenyl-3-oxo-1,2,4-triazine linked piperazine analogs as a propitious moiety to have their valuable effect in the treatment of dementia.

4. Experimental

4.1. Chemistry

4.1.1. Instrumentation and chemicals

The ^{1}H NMR (500 MHz) and ^{13}C NMR (125 MHz) spectra were recorded on a Bruker Avance FT-NMR spectrophotometer in deuterated solvents (DMSO-d_6 and $CDCl_3$) with tetramethylsilane (TMS) as an internal reference. The spectra were measured in chemical shift (*δ*, ppm) and coupling constant (*J*, Hz). Elemental analyses (C, H, N) were performed using EXETER CE-440 elemental analyzer. All the chemicals and solvents were bought from Sigma-Aldrich, TCI chemicals, Avra synthesis, and were used without further purification. Progress of chemical reactions was monitored on $60F_{254}$ sheets, precoated with silica gel, thickness- 0.25 mm, Merck, Germany. Product quantities were unoptimized which was presented in the experimental section.

4.1.2. Synthesis of intermediate (4)

Compound **4** was synthesized according to previously reported procedures [30].

*4.1.3. **General procedure of synthesis of intermediates (5, 6, 7,** and **8)***

The intermediate **4** (10 mmol) was dissolved in 20 ml of dry N,N-Dimethylformamide (DMF) in round bottom flask under the inert gas condition and stirred at 10–15 °C on ice-cold bath for 5 min. Accurate quantity (14.10 mmol) of potassium hydroxide (KOH) was added, and precipitation of compound **4** in the form of potassium salt was observed after the 30 min. The reaction mixture was kept at room temperature and bromochloro alkane (13.08 mmol) was added very slowly. After completion of reaction, DMF was evaporated under vacuo to afford the crude product, which was dissolved in ethyl acetate, washed with water (2 × 100 ml) and passed through the anhydrous sodium sulfate (Na_2SO_4) to remove the residual water. The solvent was evaporated to obtain a crude mixture, which was purified using the silica gel (100–200 mesh size) as the stationary phase and dichloromethane: methanol (4:1) as mobile phase through glass column chromatography to afford intermediates **(5, 6, 7,** and **8)**.

5,6-diphenyl-3-oxo-2-(2-chloroethyl)-(2H)-1,2,4-triazine (5)

Yield: 82%.^{1}H NMR (500 MHz, δ_H, $CDCl_3$): 7.48–7.32 (m, 10H), 4.53 (t, 2H, *J* = 7.0 Hz), 3.74 (t, 2H, *J* = 6.3 Hz). ^{13}C NMR (125 MHz, δ_C, $CDCl_3$): 166.4, 153.4, 142.2, 134.1, 133.1, 131.2, 129.8, 129.4, 128.7, 128.5, 128.3, 49.8, 41.0. Anal. $C_{17}H_{14}ClN_3O$: C, 65.49; H, 4.53; N, 13.48; Found: C, 65.39; H, 4.51; N, 13.50.

5,6-diphenyl-3-oxo-2-(3-chloropropyl)-(2H)-1,2,4-triazine (6)

Yield: 81%.^{1}H NMR (500 MHz, δ_H, $CDCl_3$): 7.49–7.30 (m, 10H), 4.44 (t, 2H, *J* = 7.0 Hz), 3.69 (t, 2H, *J* = 6.3 Hz), 2.46 (p, 2H, *J* = 6.5 Hz). ^{13}C NMR (125 MHz, δ_C, $CDCl_3$): 166.5, 153.2, 142.6, 134.9, 133.5, 131.5, 129.8, 129.3, 128.8, 128.5, 128.2, 50.9, 41.8, 30.8. Anal. $C_{18}H_{16}ClN_3O$: C, 66.36; H, 4.95; N, 12.90; Found: C, 66.39; H, 4.93; N, 12.92.

5,6-diphenyl-3-oxo-2-(4-chlorobutyl)-(2H)-1,2,4-triazine (7)

Yield: 86%. ^{1}H NMR (500 MHz, δ_H, $CDCl_3$): 7.51–7.28 (m, 10H), 4.32 (t, 2H, *J* = 7.0 Hz), 3.64 (t, 2H, *J* = 6.5 Hz), 3.50 (t, 1H, *J* = 6.8 Hz), 2.17–2.11 (m, 2H), 2.05–1.99 (m, 1H). ^{13}C NMR (125 MHz, δ_C, $CDCl_3$): 166.3, 153.3, 142.5, 134.9, 133.0, 131.4, 129.9, 129.3, 128.8, 128.5, 128.2, 52.3, 44.2, 29.5, 25.6. Anal. $C_{19}H_{18}ClN_3O$: C, 67.16; H, 5.34; N, 12.37; Found: C, 67.20; H, 5.31; N, 12.39.

5,6-diphenyl-3-oxo-2-(5-chloropentyl)-(2H)-1,2,4-triazine (8)

Yield: 84%. ^{1}H NMR (500 MHz, δ_H, $CDCl_3$): 7.51–7.29 (m, 10H), 4.29 (t, 2H, J = 7.0 Hz), 3.58 (t, 1H, J = 6.0, 6.5 Hz), 3.45 (t, 1H, J = 6.3 Hz), 1.99 (q, 2H, J = 7.5 Hz), 1.88 (t, 1H, J = 7.0), 1.71–1.61 (m, 3H). ^{13}C NMR (125 MHz, δ_C, $CDCl_3$): 166.2, 153.3, 142.4, 135, 134.1, 131.4, 129.9, 129.3, 128.8, 128.5, 128.2, 53.0, 44.7, 32.0, 27.4, 23.9. Anal. $C_{20}H_{20}ClN_3O$: C, 67.89; H, 5.70; N, 11.89; Found: C, 67.91; H, 5.67; N, 11.92.

4.1.4. General procedure of synthesis of compounds (5a-g, 6a-g, 7a-g, and 8a-g)

5.13 mmol of intermediates **(5, 6, 7,** and **8)** and various piperazine substituents (6.64 mmol), potassium iodide (7.51 mmol) and anhydrous potassium carbonate (7.51 mmol) were suspended into the dry acetonitrile (20 ml) and refluxed for 13 h. The solvent was removed under reduced pressure to get the crude product. The crude product was dissolved in ethyl acetate (2 × 100 ml) and passed through anhydrous sodium sulfate (Na_2SO_4). The organic phase was removed from the crude mixture and further purified by column chromatography on 100–200 mesh size silica gel using dichloromethane: methanol (4:1) as the mobile phase to afford pure compounds **(5a-g, 6a-g 7a-g,** and **8a-g)**.

5,6-diphenyl-3-oxo-2-(2-(4-phenylpiperazin-1-yl)ethyl)-1,2,4-triazine (5a)

Yield: 71%, ^{1}H NMR (500 MHz, δ_H, $CDCl_3$): 7.43–7.29 (m, 12H), 6.96–6.84 (m, 3H), 4.31 (t, 2H, J = 7.0 Hz), 3.35 (t, 2H, J = 5.0 Hz), 2.89–2.78 (m, 4H), 2.68–2.61 (m, 4H); ^{13}C NMR (125 MHz, δ_C, $CDCl_3$): 166.1, 153.1, 143.0, 133.9, 133.1, 131.3, 129.1, 129.2, 129.1, 128.5, 128.1, 120.1, 116.2, 54.2, 52.3, 51.5, 48.3. Anal. $C_{27}H_{27}N_5O$: C, 74.12; H, 6.22; N, 16.01; Found: C, 74.15; H, 6.20; N, 16.04.

5,6-diphenyl-3-oxo-2-(2-(4-(*p*-nitrophenyl)piperazin-1-yl) ethyl)-1,2,4-triazine (5b)

Yield: 77%. ^{1}H NMR (500 MHz, δ_H, DMSO-d_6): 8.05–8.01 (m, 4H), 7.49–7.24 (m, 6H), 7.11–6.92 (m, 4H), 4.39–4.21 (m, 2H), 3.43–3.36 (m, 2H), 2.87–2.77 (m, 4H), 2.67–2.58 (m, 4H); ^{13}C NMR (125 MHz, δ_C, DMSO-d_6): 166.3, 155.2, 149.9, 142.4, 139.7, 137.6, 137.1, 135.3, 129.2, 128.4, 128.1, 127.9, 127.8, 126.1, 113.5, 112.5, 112.7, 57.1, 52.4, 48.4, 46.1, 45.3 Anal. $C_{27}H_{26}N_6O_3$: C, 67.21; H, 5.43; N, 17.42; Found: C, 67.19; H, 5.45; N, 17.40.

5,6-diphenyl-3-oxo-2-(2-(4-(*p*-fluorophenyl)piperazin-1-yl) ethyl)-1,2,4-triazine (5c)

Yield: 69%. ^{1}H NMR (500 MHz, δ_H, $CDCl_3$): 7.49–7.29 (m, 10H), 6.95–6.91 (m, 2H), 6.88–6.81 (m, 2H), 4.35 (t, 2H, J = 7.0 Hz), 3.24–3.11 (m, 4H), 2.81–2.54 (m, 6H). ^{13}C NMR (125 MHz, δ_C, $CDCl_3$): 166.3, 157.9 (J_{CF} = 241 Hz), 153.2, 147.2, 142.1, 135.1, 134.3, 131.2, 129.8, 129.1, 128.7, 128.4, 128.1, 117.6 (J_{CF} = 23 Hz), 115.3 (J_{CF} = 8.8 Hz), 55.3, 53.2, 52.1, 49.1. Anal. $C_{27}H_{26}FN_5O$: C, 71.19; H, 5.75; N, 15.37; Found: C, 71.21; H, 5.77; N, 15.35.

5,6-diphenyl-3-oxo-2-(2-(4-(pyridin-2-yl)piperazin-1-yl)ethyl)-1,2,4-triazine (5d)

Yield: 74%. ^{1}H NMR (500 MHz, δ_H, $CDCl_3$): 8.31 (m, 1H), 7.50–7.26 (m, 11H), 6.72–6.62 (m, 2H), 4.33 (t, 2H, J = 7.3 Hz), 3.41–3.31 (m, 4H), 2.86–2.41 (m, 6H). ^{13}C NMR (125 MHz, δ_C, $CDCl_3$): 166.1, 159.2, 153.2, 147.9, 142.2, 137.4, 135.2, 134.3, 131.4, 129.7, 129.1, 128.8, 128.4, 128.1, 113.1, 107.1, 58.3, 53.0, 45.1, 28.2. Anal. $C_{26}H_{26}N_6O$: C, 71.21; H, 5.98; N, 19.16; Found: 71.24; H, 5.96; N, 19.18.

5,6-diphenyl-3-oxo-2-(2-(4-(*p*-methoxyphenyl)piperazin-1-yl) ethyl)-1,2,4-triazine (5e)

Yield: 67%. ^{1}H NMR (500 MHz, δ_H, DMSO-d_6): 7.51–7.28 (m, 10H), 6.85–6.72 (m, 4H), 4.32 (t, 2H, J = 7.3 Hz), 3.71 (s, 3H, –OCH_3), 3.56–3.40 (m, 2H), 2.87–2.71 (m, 4H), 2.65–2.51 (m, 4H). ^{13}C NMR (125 MHz, δ_C, DMSO-d_6): 166.4, 153.3, 153.1, 144.6, 142.2, 135.8, 134.1, 130.3, 129.7, 129.3, 129.3, 128.5, 128.4, 117.3, 114.7, 57.2, 55.4, 53.1, 52.2, 49.6. Anal. $C_{28}H_{29}N_5O_2$: C, 71.93; H, 6.25; N, 14.98; Found: C, 71.95; H, 6.21a; N, 15.00.

5,6-diphenyl-3-oxo-2-(2-(4-benzhydrylpiperazin-1-yl)ethyl)-1,2,4-triazine (5f)

Yield: 73%. ^{1}H NMR (500 MHz, δ_H, $CDCl_3$): 7.56–7.15 (m, 20H), 4.29 (t, 2H, J = 6.8 Hz), 4.11 (s, 1H), 3.52–3.41 (m, 4H), 2.84–2.73 (m, 4H), 2.61–2.54 (m, 2H). ^{13}C NMR (125 MHz, δ_C, $CDCl_3$): 166.1, 153.1, 143.0, 142.3, 134.9, 134.1, 131.2, 130.0, 130.2, 128.7, 128.3, 128.0, 126.5, 76.4, 55.3, 53.2, 52.1. Anal. $C_{34}H_{33}N_5O$: C, 77.39; H, 6.30; N, 13.27; Found: C, 77.45; H, 6.27; N, 13.31.

5,6-diphenyl-3-oxo-2-(2-(4-benzylpiperazin-1-yl)ethyl)-1,2,4-triazine (5g)

Yield: 73%. ^{1}H NMR (500 MHz, δ_H, $CDCl_3$): 7.50–7.12 (m, 15H), 4.33 (t, 2H, J = 7.0 Hz), 3.45–3.38 (m, 6H), 2.87–2.72 (m, 4H), 2.67–2.56 (m, 2H). ^{13}C NMR (125 MHz, δ_C, $CDCl_3$): 166.2, 153.4, 143.1, 142.31 134.9, 134.3, 131.2, 130.5, 130.1, 128.3, 128.1, 128.0, 126.4, 62.9, 55.5, 53.4, 52.5, 48.9. Anal. $C_{28}H_{29}N_5O$: C, 74.47; H, 6.47; N, 15.51; Found: C, 74.53; H, 6.45; N, 15.48.

5,6-diphenyl-3-oxo-2-(3-(4-phenylpiperazin-1-yl)propyl)-1,2,4-triazine (6a)

Yield: 70%, ^{1}H NMR (500 MHz, δ_H, $CDCl_3$): 7.43–7.24 (m, 12H), 6.91–6.86 (m, 3H), 4.33 (t, 2H, J = 7.0 Hz), 3.25 (t, 4H, J = 5.0 Hz), 2.88 (d, 4H, J = 5.0 Hz), 2.79 (t, 2H, J = 7.3 Hz), 2.27 (t, 2H, J = 7.3 Hz). ^{13}C NMR (125 MHz, δ_C, $CDCl_3$): 166.5, 153.2, 142.7, 134.9, 134.0, 131.4, 129.8, 129.3, 129.1, 128.5, 128.2, 120.3, 116.4, 54.8, 52.2, 51.4, 48.2, 29.3. Anal. $C_{18}H_{16}ClN_3O$: C, 74.47; H, 6.47; N, 15.51; Found: C, 74.51; H, 6.43; N, 15.50.

5,6-diphenyl-3-oxo-2-(3-(4-(*p*-nitrophenyl)piperazin-1-yl) propyl)-1,2,4-triazine (6b)

Yield: 74%. ^{1}H NMR (500 MHz, δ_H, $CDCl_3$): 8.11–8.09 (m, 1H), 7.47–7.15 (m, 12H), 6.79–6.78 (m, 1H), 4.49–4.37 (m, 3H), 3.38 (s, 2H), 2.72–2.60 (m, 5H), 2.32–2.02 (m, 3H), 1.63–1.61 (m, 1H); ^{13}C NMR (125 MHz, δ_C, $CDCl_3$): 166.6, 154.8, 149.2, 142.8, 139.2, 137.6, 137.1, 135.3, 129.8, 128.8, 128.5, 127.9, 127.8, 125.9, 114.0, 112.6, 55.4, 52.4, 51.0, 46.1, 29.6; Anal. $C_{28}H_{28}N_6O_3$: C, 67.73; H, 5.68; N, 16.92; Found: C, 67.76; H, 5.65; N, 16.96.

5,6-diphenyl-3-oxo-2-(3-(4-(*p*-fluorophenyl)piperazin-1-yl) propyl)-1,2,4-triazine (6c)

Yield: 71%. ^{1}H NMR (500 MHz, δ_H, $CDCl_3$): 7.41–7.26 (m, 10H), 6.95–6.92 (m, 2H), 6.84–6.82 (m, 2H), 4.37 (t, 2H, J = 7.0 Hz), 3.06 (t, 4H, J = 4.5 Hz), 2.61–2.57 (m, 6H), 2.30–2.17 (m, 6H, J = 6.8 Hz). ^{13}C NMR (125 MHz, δ_C, $CDCl_3$): 166.2, 156.1, 153.4, 147.9, 142.2, 135.0, 134.1, 131.3, 129.8, 129.2, 128.8, 128.5, 128.1, 117.8 ($J_{CF\text{-}O}$ = 30.0 Hz), 115.5 ($J_{CF\text{-}m}$ = 88.5 Hz), 55.6, 53.1, 52.0, 50.2, 25.2; Anal. $C_{28}H_{28}FN_5O$: C, 71.62; H, 6.01; N, 14.91; Found: C, 71.65; H, 6.03; N, 14.94.

5,6-diphenyl-3-oxo-2-(3-(4-(pyridin-2-yl)piperazin-1-yl) propyl)-1,2,4-triazine (6d)

Yield: 75%. ^{1}H NMR (500 MHz, δ_H, $CDCl_3$): 8.17 (s, 1H), 7.47–7.25 (m, 11H), 6.62–6.60 (d, 2H, J = 7.0 Hz), 4.36 (t, 2H, J = 6.5 Hz), 3.50 (s, 4H), 2.57 (s, 6H), 2.18 (t, 2H, J = 6.8 Hz). ^{13}C NMR (125 MHz, δ_C, $CDCl_3$): 166.2, 159.4, 153.4, 147.8, 142.3, 137.4, 135.0, 134.1, 131.3, 129.8, 129.2, 128.8, 128.5, 128.1, 113.3, 107.1, 55.6, 52.9, 51.9, 45.2, 29.6; Anal. $C_{27}H_{28}N_6O$: C, 71.66; H, 6.24; N, 18.57; Found: C, 71.70; H, 6.25; N, 18.59.

5,6-diphenyl-3-oxo-2-(3-(4-(*p*-methoxyphenyl)piperazin-1-yl) propyl)-1,2,4-triazine (6e)

Yield: 72%. ^{1}H NMR (500 MHz, δ_H, $CDCl_3$): 7.47–7.24 (m, 10H), 6.85–6.79 (m, 4H), 4.34 (t, 2H, J = 6.5 Hz), 3.73 (s, 3H, -OCH_3), 3.03 (brs, 4H), 2.60–2.56 (m, 6H), 2.16 (t, 2H, J = 6.8 Hz). ^{13}C NMR (125 MHz, δ_C, $CDCl_3$): 166.2, 153.7, 153.4, 145.6, 142.3, 135.0, 134.1, 131.3, 129.8, 129.2, 128.9, 128.8, 128.5, 128.1, 118.2, 114.3, 55.6, 55.5, 53.2, 52.0, 50.6, 25.2; Anal. $C_{29}H_{31}N_5O_2$: C, 72.33; H, 6.49; N, 14.54; Found: C, 72.35; H, 6.46; N, 14.53.

5,6-diphenyl-3-oxo-2-(3-(4-benzhydrylpiperazin-1-yl)propyl)-1,2,4-triazine (6f)

Yield: 72%. ^{1}H NMR (500 MHz, δ_H, $CDCl_3$): 7.53–7.16 (m, 20H), 4.33 (t, 2H, J = 7.0 Hz), 4.13 (s, 1H), 2.55–2.38 (m, 9H), 2.13 (q, 2H, J = 6.9 Hz), 1.68 (s, 1H). ^{13}C NMR (125 MHz, δ_C, $CDCl_3$): 166.0, 153.4,

142.8, 142.1, 135.1, 134.2, 131.3, 129.9, 129.1, 128.8, 128.4, 128.1, 127.9, 126.8, 76.3, 55.6, 53.3, 52.0, 25.3. Anal. $C_{35}H_{35}N_5O$: C, 77.60; H, 6.51; N, 12.93; Found: C, 77.63; H, 6.53; N, 12.90.

5,6-diphenyl-3-oxo-2-(3-(4-benzylpiperazin-1-yl)propyl)-1,2,4-triazine (6g)

Yield: 72%. ^{1}H NMR (500 MHz, δ_H, $CDCl_3$): 7.50–7.22 (m, 15H), 4.31 (brs, 2H), 3.44 (brs, 2H), 2.51–2.45 (m, 8H), 2.12–2.02 (m, 2H), 1.42–1.37 (m, 2H). ^{13}C NMR (125 MHz, δ_C, $CDCl_3$): 166.1, 153.4, 142.2, 139.2, 137.8, 135.0, 134.1, 131.3, 129.9, 129.2, 128.8, 128.5, 127.0, 114.1, 62.9, 55.6, 52.9, 52.0, 29.7. Anal. $C_{35}H_{35}N_5O$: C, 77.60; H, 6.51; N, 12.93; Found: C, 77.63; H, 6.53; N, 12.90.

5,6-diphenyl-3-oxo-2-(4-(4-phenylpiperazin-1-yl)butyl)-1,2,4-triazine (7a)

Yield: 60%. ^{1}H NMR (500 MHz, δ_H, $CDCl_3$): 7.51–7.26 (m, 12H), 6.94 (d, 2H, J = 7.5 Hz), 6.94 (t, 1H, J = 7.0 Hz), 4.32 (t, 2H, J = 6.8 Hz), 3.21 (m, 4H), 2.62 (m, 4H), 2.49 (t, 2H, J = 7.5 Hz), 2.02 (t, 2H, J = 6.8 Hz), 1.28 (m, 2H). ^{13}C NMR (100 MHz, δ_C, $CDCl_3$): 166.2, 153.3, 151.3, 142.4, 135.0, 134.1, 131.4, 129.9, 129.2, 129.1, 128.9, 128.5, 128.2, 58.0, 53.4, 53.2, 53.0, 49.1, 26.2, 23.9. Anal. $C_{29}H_{31}N_5O$: C, 74.81; H, 6.71; N, 15.04; Found: C, 74.83; H, 6.69; N, 15.05.

5,6-diphenyl-3-oxo-2-(4-(4-(*p*-nitrophenyl)piperazin-1-yl) butyl)-1,2,4-triazine (7b)

Yield: 79%. ^{1}H NMR (500 MHz, δ_H, DMSO-d_6): 8.08 (d, 2H, J = 9.5 Hz), 8.05 (d, 2H, J = 9.5 Hz),7.45 (d, 2H, J = 7.5 Hz), 7.24–7.20 (m, 4H), 7.08 (d, 2H, J = 9.0 Hz), 6.98 (d, 2H, J = 9.5 Hz), 3.67 (s, 4H), 3.40–3.34 (m, 4H), 2.76 (s, 4H), 2.50–2.46 (m, 4H). ^{13}C NMR (125 MHz, δ_C, DMSO-d_6): δ 166.2, 155.1, 150.2, 142.9, 139.9, 137.5, 137.3, 135.7, 129.2, 128.8, 128.7, 128.1, 128.0, 126.1, 113.1, 112.9, 112.8, 57.3, 52.7, 48.3, 46.7, 45.7, 26.5, 23.6. Anal. $C_{29}H_{30}N_6O_3$: C, 68.29; H, 5.92; N, 16.46; Found: C, 68.32; H, 5.93; N, 16.48.

5,6-diphenyl-3-oxo-2-(4-(4-(*p*-fluorophenyl)piperazin-1-yl) butyl)-1,2,4-triazine (7c)

Yield: 68%. ^{1}H NMR (500 MHz, δ_H, $CDCl_3$): 7.51–7.29 (m, 10H), 6.98–6.86 (m, 4H), 4.31 (t, 2H, J = 7.0 Hz), 3.12 (m, 4H), 2.49 (t, 4H, J = 7.0 Hz), 2.03 (t, 2H, J = 7.0 Hz), 1.68 (m, 2H) 1.27 (m, 2H). ^{13}C NMR (125 MHz, δ_C, $CDCl_3$): δ 166.2, 158.0, 156.2, 153.3, 147.9, 142.4, 134.9, 134.1, 131.4, 129.8, 128.9, 128.5, 128.2, 117.8, 117.7, 115.5, 115.4, 57.9, 53.2, 50.0, 26.2, 23.8. Anal. $C_{29}H_{30}FN_5O$: C, 72.03; H, 6.25; N, 14.48; Found: C, 72.01; H, 6.29; N, 14.41.

5,6-diphenyl-3-oxo-2-(4-(4-(pyridin-2-yl)piperazin-1-yl)butyl)-1,2,4-triazine (7d)

Yield: 76%. ^{1}H NMR (500 MHz, δ_H, $CDCl_3$): 8.31 (m, 1H), 7.51–7.28 (m, 11H), 6.66–6.62 (m, 2H), 4.32 (t, 2H, J = 7.3 Hz), 3.55 (t, 4H, J = 4.5 Hz), 2.57 (t, 4H, J = 4.5 Hz), 2.48 (t, 2H, J = 7.5 Hz), 2.03 (q, 2H, J = 7.3 Hz), 1.73–1.67 (m, 2H). ^{13}C NMR (125 MHz, δ_C, $CDCl_3$): 166.2, 159.5, 153.3, 147.9, 142.4, 137.4, 135.0, 134.1, 131.3, 129.8, 129.2, 128.9, 128.5, 128.2, 113.2, 107.0, 58.1, 53.0, 45.1, 26.2, 23.8. Anal. $C_{28}H_{30}N_6O$: C, 72.08; H, 6.48; N, 18.01; Found: C, 72.10; H, 6.44; N, 18.03.

5,6-diphenyl-3-oxo-2-(4-(4-(*p*-methoxyphenyl)piperazin-1-yl) butyl)-1,2,4-triazine (7e)

Yield: 74%. ^{1}H NMR (500 MHz, δ_H, H, DMSO-d_6): 7.48–7.29 (m, 10H), 6.86–6.79 (m, 4H), 4.17 (t, 2H, J = 7.3 Hz), 3.67 (s, 3H, –OCH_3), 2.97 (s, 4H), 2.51–2.47 (m, 4H), 2.37 (t, 2H, J = 7.3 Hz), 1.87 (t, 2H, J = 7.3 Hz), 1.56 (t, 2H, J = 7.3 Hz). ^{13}C NMR (125 MHz, δ_C, DMSO-d_6): δ 166.3, 153.2, 152.9, 145.9, 142.3, 135.8, 134.7, 131.3, 129.8, 129.4, 129.3, 128.6, 128.5, 117.6, 114.6, 57.7, 55.6, 53.3, 52.6, 50.0, 26.0, 23.7. Anal. $C_{30}H_{33}N_5O_2$: C, 72.70; H, 6.71; N, 14.13; Found: C, 72.67; H, 6.74; N, 14.11.

5,6-diphenyl-3-oxo-2-(4-(4-benzhydrylpiperazin-1-yl)butyl)-1,2,4-triazine (7f)

Yield: 81%. ^{1}H NMR (500 MHz, δ_H, $CDCl_3$): δ 7.49–7.13 (m, 20H), 4.26–4.22 (m, 2H), 4.11 (s, 1H), 3.07 (brs, 8H), 2.40 (brs, 2H), 1.95 (brs, 2H), 1.59–1.28 (m, 2H). ^{13}C NMR (125 MHz, δ_C, $CDCl_3$): 166.1, 153.3, 142.7, 142.3, 135.0, 134.1, 131.3, 130.0, 129.8, 129.2, 128.9, 128.4, 128.2, 127.9, 126.9, 76.2, 57.9, 53.4, 53.0, 51.8, 26.1, 23.8. Anal. $C_{36}H_{37}N_5O$: C, 77.81; H, 6.71; N, 12.60; Found: C, 77.79; H, 6.73; N, 12.64.

5,6-diphenyl-3-oxo-2-(4-(4-benzylpiperazin-1-yl)butyl)-1,2,4-triazine (7g)

Yield: 81%. ^{1}H NMR (500 MHz, δ_H, $CDCl_3$): 7.43–7.24 (m, 15H), 4.23 (t, 2H, J = 6.5 Hz), 3.46–3.19 (m, 4H), 2.38 (brs, 8H), 1.92 (brs, 2H), 1.58 (brs, 2H). ^{13}C NMR (125 MHz, δ_C, $CDCl_3$): 166.1, 153.3, 142.3, 137.9, 134.9, 134.0, 131.3, 129.8, 129.2, 129.0, 128.8, 128.4, 128.1, 127.7, 127.2, 127.0, 63.0, 57.9, 53.1, 53.0, 52.9, 26.1, 23.8. Anal. $C_{30}H_{33}N_5O$: C, 75.13; H, 6.94; N, 14.60; Found: C, 75.08; H, 6.97; N, 14.63.

5,6-diphenyl-3-oxo-2-(5-(4-phenylpiperazin-1-yl)pentyl)-1,2,4-triazine (8a)

Yield: 72%. ^{1}H NMR (500 MHz, δ_H, $CDCl_3$): 7.51–7.26 (m, 12H), 6.94 (d, 2H, J = 8.0 Hz), 6.86 (t, 1H, J = 6.8 Hz), 4.29 (t, 2H, J = 7.0 Hz), 3.21 (s, 4H), 2.61 (s, 4H), 2.43 (t, 2H, J = 7.0 Hz), 2.00 (t, 2H, J = 6.8 Hz), 1.64 (d, 2H, J = 6.0 Hz), 1.51 (d, 2H, J = 6.5 Hz). ^{13}C NMR (125 MHz, δ_C, $CDCl_3$): 166.2, 153.3, 151.3, 142.3, 135.0, 134.1, 131.4, 129.9, 129.2, 129.1, 128.9, 128.5, 128.2, 119.6, 116.0, 58.4, 53.2, 49.1, 28.1, 26.4, 24.6. Anal. $C_{30}H_{33}N_5O$: C, 75.13; H, 6.94; N, 19.97; Found: C, 75.11; H, 6.93; N, 19.99.

5,6-diphenyl-3-oxo-2-(5-(4-(*p*-nitrophenyl)piperazin-1-yl) pentyl)-1,2,4-triazine (8b)

Yield: 76%. ^{1}H NMR (500 MHz, δ_H, DMSO-d_6): 8.08–8.01 (m, 4H), 7.45–7.08 (m, 8H), 6.98–6.89 (m, 2H), 3.67–3.59 (m, 2H), 3.27–3.21 (m, 4H), 2.61–2.48 (m, 4H), 2.21–2.01 (m, 4H), 1.66–1.51 (m, 2H), 1.39–1.28 (m, 2H). ^{13}C NMR (125 MHz, δ_C, DMSO-d_6): 166.2, 155.1, 150.2, 142.9, 139.9, 137.5, 137.3, 135.7, 129.2, 128.8, 128.7, 128.1, 128.0, 126.1, 113.1, 112.9, 112.8, 57.3, 52.7, 48.3, 28.2, 26.5, 23.6. Anal. $C_{30}H_{32}N_6O_3$: C, 68.68; H, 6.15; N, 16.02; Found: C, 68.71; H, 6.11; N, 16.04.

5,6-diphenyl-3-oxo-2-(5-(4-(*p*-fluorophenyl)piperazin-1-yl) pentyl)-1,2,4-triazine (8c)

Yield: 71%. ^{1}H NMR (500 MHz, δ_H, $CDCl_3$): 7.51–7.26 (m, 10H), 6.97–6.86 (m, 4H), 4.32 (t, 2H, J = 7.0 Hz), 3.14 (m, 4H), 2.43 (t, 4H, J = 6.8 Hz), 2.32–1.89 (m, 4H), 1.68–1.53 (m, 2H) 1.39–1.27 (m, 2H). ^{13}C NMR (125 MHz, δ_C, $CDCl_3$): 166.4, 157.9, 156.0, 153.2, 147.6, 142.2, 134.7, 134.1, 131.3, 129.9, 128.5, 128.3, 128.1, 117.9, 117.2, 115.4, 115.2, 57.2, 53.1, 50.3, 28.4, 26.1, 23.2. Anal. $C_{30}H_{32}FN_5O$: C, 72.41; H, 6.48; N, 14.07; Found: C, 72.39; H, 6.51; N, 14.10.

5,6-diphenyl-3-oxo-2-(5-(4-(pyridin-2-yl)piperazin-1-yl) pentyl)-1,2,4-triazine (8d)

Yield: 63%. ^{1}H NMR (500 MHz, δ_H, $CDCl_3$): 8.31 (m, 1H), 7.52–7.26 (m, 11H), 6.65–6.62 (m, 2H), 4.32 (t, 2H, J = 7.0 Hz), 3.54 (t, 4H, J = 4.5 Hz), 2.54–2.44 (m, 4H), 2.33–1.98 (m, 4H), 1.72–1.67 (m, 2H), 1.37–1.28 (m, 2H). ^{13}C NMR (125 MHz, δ_C, $CDCl_3$): 166.1, 159.2, 153.1, 147.2, 142.4, 137.4, 135.1, 134.2, 131.3, 129.7, 129.1, 128.8, 128.5, 128.3, 113.1, 107.1, 58.3, 52.9, 45.5, 28.3, 26.0, 23.5. Anal. $C_{29}H_{32}N_6O$: C, 72.47; H, 6.71; N, 17.49; Found: C, 72.51; H, 6.69; N, 17.51.

5,6-diphenyl-3-oxo-2-(5-(4-(*p*-methoxyphenyl)piperazin-1-yl) pentyl)-1,2,4-triazine (8e)

Yield: 66%. ^{1}H NMR (500 MHz, δ_H, DMSO-d_6): 7.47–7.26 (m, 10H), 6.86–6.78 (m, 4H), 4.21 (t, 2H, J = 7.3 Hz), 3.62 (s, 3H, -OCH_3), 3.25–3.14 (m, 4H), 2.52–2.39 (m, 4H), 2.31–2.01 (m, 4H), 1.89–1.67 (m, 2H), 1.56–1.30 (m, 2H). ^{13}C NMR (125 MHz, δ_C, DMSO-d_6): 166.3, 153.1, 152.9, 145.8, 142.1, 135.2, 134.6, 131.4, 129.8, 129.4, 129.3, 128.4, 128.5, 117.7, 114.4, 57.1 55.6, 53.1, 52.6, 50.2, 28.3, 26.1, 23.7. Anal. $C_{31}H_{35}N_5O_2$: C, 73.06; H, 6.92; N, 13.74; Found: C, 73.03; H, 6.93; N, 13.77.

5,6-diphenyl-3-oxo-2-(5-(4-benzhydrylpiperazin-1-yl)pentyl)-1,2,4-triazine (8f)

Yield: 72%. ^{1}H NMR (500 MHz, δ_H, $CDCl_3$): 7.53–7.14 (m, 20H), 4.34 (t, 2H, J = 6.8 Hz), 4.12 (s, 1H), 2.87–2.54 (m, 4H), 2.43–2.32 (m,

6H), 2.11–2.01 (m, 2H), 1.61–1.48 (m, 2H), 1.39–1.31 (m, 2H). ^{13}C NMR (125 MHz, δ_C, $CDCl_3$): 166.2, 153.3, 142.8, 142.3, 135.2, 134.1, 131.3, 129.9, 129.1, 128.7, 128.2, 128.3, 127.8, 126.6, 76.3, 55.3, 53.4, 52.1, 28.1, 26.3, 23.2. Anal. $C_{37}H_{39}N_5O$: C, 78.00; H, 6.90; N, 12.29; Found: C, 78.05; H, 6.93; N, 12.31.

5,6-diphenyl-3-oxo-2-(5-(4-benzylpiperazin-1-yl)pentyl)-1,2,4-triazine (8g)

Yield: 72%. ^{1}H NMR (500 MHz, δ_H, $CDCl_3$): 7.45–7.21 (m, 15H), 4.21 (t, 2H, J = 6.5 Hz), 3.44–3.23 (m, 4H), 2.38–2.31 (m, 8H), 1.92 (brs, 2H), 1.58–1.45 (m, 2H), 1.42–1.34 (m, 2H). ^{13}C NMR (125 MHz, δ_C, $CDCl_3$): 166.2, 153.2, 142.1, 137.6, 134.9, 134.2, 131.1, 129.9, 129.5, 129.1, 128.8, 128.2, 128.6, 127.4, 127.2, 126.9, 63.2, 57.4, 53.3, 53.0, 53.0, 29.7, 26.4, 23.8. Anal. $C_{31}H_{35}N_5O$: C, 75.43; H, 7.15; N, 14.19; Found: C, 75.39; H, 7.11; N, 14.23.

4.2. Pharmacology

4.2.1. In vitro cholinesterase inhibition assay

The cholinesterase inhibitory potency of synthesized derivatives was evaluated against the AChE and BChE as per the Ellman protocol [54,55]. All the tested compounds were dissolved in DMSO to prepare the stock solutions and their dilutions were made in eight different concentrations (10 nM to 100 μM). A solution of 2.5 units/ml of cholinesterase (*electric eel* AChE or *equine serum* BChE) was prepared in 0.1 M sodium phosphate buffer pH 7.4.

In the 96-well microplate, 25 μL solutions of respective cholinesterase enzymes (AChE and BChE) and 10 μL of test compounds were incubated for 10 min at room temperature. Further, 240 μL of 0.1 M of sodium phosphate buffer, 40 μL of 1 mM 5,5′-Dithiobis-2-nitrobenzoic acid (DTNB) and 10 μL of 7.5 mM substrate acetylthiocholine iodide (ATCI) or butyrylthiocholine iodide (BTCI) were added. The enzymatic and non-enzymatic reactions were allowed to continue at time intervals for 10 min, and absorbance was measured in triplicate at a wavelength of 412 nm. The change in the rate of reaction and the percentage of AChE or BChE inhibitory potency were assessed, and the IC_{50} value was calculated using Graph Pad Prism 5.

The enzyme kinetics study was executed to assess the type of AChE inhibition from all synthesized compounds. The varying concentrations of ATCI were prepared in the 0.1 M of phosphate buffer at pH 7.4. The AChE and various concentrations of prepared ATCI solutions were mixed and incubated in the presence or absence of compounds, and then absorption was recorded at 412 nm. Finally, kinetics of AChE inhibition was determined by Lineweaver and Burk procedure [56].

4.2.2. In vitro propidium iodide displacement assay

The five units of AChE enzyme solution were prepared in the tris (hydroxymethyl)aminomethane buffer pH 8.0 and added into the 96-well plate. 150 μL of different concentrations (50 μM and 30 μM) of synthesized compounds and standard donepezil solutions were added in the well and incubated for 6 h at 25 °C. After 6 h, 20 μL of 1 μM propidium iodide solution was incubated for 10 min at room temperature. The fluorescence intensity was recorded at an excitation wavelength (λ_{ex} = 535 nm) and emission (λ_{em} = 595 nm) in the microplate reader (Synergy H1M, Biotek) [48].

4.2.3. PAMPA-BBB assay

The permeability of test compounds is determined by PAMPA-BBB assay [49]. The filter membrane was coated with 4 μL of porcine brain lipid (PBL), and acceptor plate was filled with 200 μL of phosphate saline buffer: ethanol (70:30) solution. The stock solutions (5 mg/ml) of test compounds were prepared in DMSO. The 10 μL of the stock solution was further diluted with phosphate saline buffer: ethanol (70:30) up to 200 folds that resulted in secondary stock solutions (25 μg/ml). The 200 μL of these secondary stock solutions were added into the donor microplate. The acceptor microplate was sandwiched on donor plate and incubated for 20 h at 25 °C. The concentration of test compounds and standard drugs were analyzed by recording the absorbance in triplicates.

4.2.4. Neurotoxicity assay by SH-SY5Y neuroblastoma cell

The neurotoxic effect of the hybrid compound **6g** was determined on neuroblastoma cell lines SH-SY5Y by MTT assay [50,57]. SH-SY5Y cell lines (density of 1×10^5 cells/well) were seeded on 96 well microplates in 100 μL of the medium and incubated for 24 h at 37 °C in 5% carbon dioxide. After 24 h, five different concentrations of test compound and standard donepezil were incubated with the neuroblastoma cells. Then, 20 μL of MTT reagent (3-(4,5-dimethylthiazol-2-yl)-2,5-diphenyl tetrazolium bromide) was added and incubated for an additional 3 h. After incubation, the formation of a purple color was observed under a microscope and solubilized in 100 μL of DMSO. The IC_{50} value was determined by measuring the absorbance at 570 nm in a microplate reader (Synergy H1M, BioTek) using Graph Pad Prism 5.01.

4.2.5. In vivo behavioral studies

4.2.5.1. Animals. *In vivo* studies were performed on adult male Swiss albino mice (25–30 gm). The mice were bought from Central Animal Breeding House, Institute of Medical Sciences (IMS), Banaras Hindu University (BHU), Varanasi, India. They were kept as groups of six per polyacrylic cage and given semi-synthetic balanced diet and water. The animals were maintained at a temperature (25 ± 2 °C) and relative humidity (55 ± 10%) with 12 h light/dark cycles. Different animals were used for each behavioral investigation. The institutional animal ethical committee duly permitted the study protocols and quantity of mice (No. Dean/2017/CAEC/94).

4.2.5.2. Material. Scopolamine hydrobromide was purchased from Sigma-Aldrich, India. The experiments were performed on the y-Maze and two-compartment passive avoidance apparatus.

4.2.5.3. Acute oral toxicity study. The compound **6g** was evaluated on healthy Swiss albino mice as per OECD-423, 2001 guidelines for acute oral toxicity. The compound **6g** was administered in doses up to 500 mg/kg, and the mice were observed regularly up to 14 consecutive days for toxic reactions or mortality [51].

4.2.5.4. Experimental strategy and drug administration protocol. Donepezil hydrochloride and compound **6g** were suspended in the 0.3% sodium carboxymethyl cellulose (CMC). The behavioural studies were performed in seven groups with each group having six mice as following: (i) control; (ii) scopolamine (0.5 mg/kg, i.p.); (iii) vehicle + scopolamine; (iv) donepezil (5 mg/kg, p.o.) + scopolamine (v) compound **6g** (2.5 mg/kg, p.o.) + scopolamine (vi) compound **6g** (5 mg/kg, p.o.) + scopolamine (vii) compound **6g** (10 mg/kg, p.o.) + scopolamine. Compound **6g** and donepezil were given once daily for seven consecutive days to their respective groups. On the 7th day of the experiment, scopolamine hydrobromide was dissolved in distilled water and administered i.p. after 30 min of drug treatment.

4.2.5.5. Y-maze test. The y-maze apparatus consists of three arms maze extensively used for the estimation of instant and short working memory in the rodents. After 30 min of 7th day treatment, scopolamine hydrobromide was administered *i.p.* to all groups of mice except the control group. The mice of each group were kept in the center of y-maze to reconnoiter the three arms for the 5 min. Activities were observed in the camera to record the total arm entries. The "memory improvement score" can be calculated as % alternations = (Number of alternations/(total arm entries – 2)) × 100 [52].

4.2.5.6. Passive avoidance experiment. The passive avoidance instrument has a fabricated box with two compartments (dark/lit; each 12 × 10 × 12 cm) connected through a door and stainless steel electric bar (2 mm) placed at a distance of 0.5 cm. The instrument has

an electronic display timer and voltage system which regulates the current flow (0.05 mA) and voltage (20 V), respectively. The experiment was performed into two separate phases: acquisition and retention test. Also, the interval between the acquisition and retention test should be at least one day. Both the tests (acquisition and retention) were performed for the total period of 300 s. The compound **6g** and donepezil were administered once daily for seven days. The experiment was performed on the 7th day of dosing. The acquisition phase was initiated after i.p. administration of scopolamine hydrobromide. After five minutes, each mouse was kept and exposed for 30 *sec* (acquisition time) in first lit chamber of two compartment instrument. The entry door of the second dark compartment was opened, and as the mouse was entered in the dark compartment, the door was locked. Next, the medium intensity of electric foot shock (0.05 mA, 2-seconds) was applied to the mice through the stainless steel electric bar in the dark compartment. Next day, the retention test was performed in which each mouse was kept in the lit chamber and observed for their entry from lit to a dark chamber within 300 s. The entry to the dark chamber was measured as transfer latency time (TLT). In the retention test, foot shock was not delivered to prevent reacquisition [58].

4.2.6. Dissection and homogenization

After the completion of the behavioral assessments, mice were forfeited through the cervical dislocation, and their whole brain was isolated, washed with cold double distilled water, and again rinsed with a pre-cooled normal saline solution. Each whole brain and 3 ml of 10 mM phosphate buffered saline (pH 7.4) were homogenized in the teflon-glass homogenizer at ice-cold bath and centrifuged at 2–8 °C for 10 min at 11,000 rpm to get the supernatant, which was used to analyze the various biochemical parameters.

4.2.7. Neurochemical estimation of AChE

The *ex vivo* study was used to govern the AChE inhibition of compound **6g**. The AChE level was evaluated according to the Ellman's assay protocol [54]. Initially, 25 µL of supernatant, 150 µL of 0.1 M sodium phosphate buffer (pH 7.4), and 100 µL of 1 mM of DTNB were added in 96 well microplate and incubated for 10 min followed by addition of 20 µL of 7.5 mM of ATCI to initiate the reaction The absorbance of the reaction mixture was measured at 412 nm. The results of AChE inhibitory potency was expressed as substrate hydrolyzed/min/mg protein.

4.2.8. Biochemical estimation of the oxidative stress factors

4.2.8.1. 2-thiobarbituric acid reactive substances (TBARS) estimation. This assay was used to evaluate the antioxidant potential on the lipid peroxidation in brain homogenate [59]. The 50 µL of supernatant and cold solution of 10% trichloroacetic acid (TCA) were mixed and centrifuged for 12 min at 1200 rpm. After centrifugation, 100 µL of the supernatant and 100 µL of 0.67% of 2-sulfanylidene-1,3-diazinane-4,6-dione (2-thiobarbituric acid) were mixed and warmed for 10 min, cooled, and followed by addition of 100 µL of double distilled water and the absorbance of the final reaction mixture was recorded at 532 nm. The intensity of the pink color of the TBARS is proportional to the level of lipid peroxidation in the homogenate. Finally, the results were articulated as the number of moles of MDA/mg protein.

4.2.8.2. Reduced glutathione assay. The supernatant (50 µL) was deproteinized by adding 4% of sulphosalicylic acid (50 µL) at 4 °C and mixed subsequently with the addition of 10 mM DTNB. The reduced glutathione was recorded at 412 nm, and the outcomes were presented as micromole of GSH/mg protein [60].

4.2.8.3. Superoxide dismutase (SOD) assay. The estimation of superoxide dismutase was performed as per the reported protocol. Primarily, the reagent was prepared by 0.1 mM of ethylenediaminetetraacetic acid (EDTA), 24 µM of nitro blue tetrazolium (NBT), and 50 mM of anhydrous sodium carbonate (Na_2CO_3). Further, 200 µL of prepared reagent, 50 µL of supernatant and 50 µL of $NH_2OH.HCl$ (hydroxylamine hydrochloride) were mixed, and the reaction mixture was maintained to pH 10.2. The auto-oxidation of $NH_2OH.HCl$ was recorded in the variation of the absorbance for 5 min at regular intervals at 560 nm [61].

4.2.8.4. Estimation of nitrite. Nitrite was assessed through the Greiss reagent from the supernatant collected from brain homogenates. Briefly, 10 ml of Griess reagent was prepared by mixing 5 ml of 1% sulphanilic acid in 2.5% concentrated phosphoric acid (H_3PO_4) and 5 ml of 0.1% of N-(1-Naphthyl)ethylenediamine dihydrochloride (NEDD) in double distilled water. Then, freshly prepared 250 µL of Griess reagent and 50 µL supernatant were added in the 96 well plates, and absorbance was recorded at 546 nm. Nitrite quantity (mg/ml) was calculated from a sodium nitrite standard curve [62].

4.2.8.5. Estimation of catalase. The assay mixture consisted of 150 µL of 10 mM sodium phosphate buffer (pH 7.4), 100 µL of 19 mM of hydrogen peroxide (H_2O_2) and 50 µL the brain supernatant. Variation in the absorbance was measured at 240 nm, and the outcomes were stated as mmoles of H_2O_2 decomposed/min/mg protein [13].

4.3. Computational studies

4.3.1. In silico docking simulations

The molecular docking studies were carried out to analyze the consensual binding and active site interactions of compound **6g** on AChE (PDB Code: 1EVE) [63]. The crystal structure of the protein was prepared using the Protein Preparation Wizard module. Initially, the hydrogen bonds and bond orders were assigned. The missing side chains and loops were added using Prime. The water molecules with more than 5 Å distance from the heteroatoms were deleted and hetero atoms states were generated using the Epik at pH 7.0 ± 2.0. Further, the protein structure was optimized by PROPKA method at pH 7.0 and minimized at restrained minimization by keeping the convergence heavy atoms RMSD to 0.30 Å. The prepared protein structure was used for receptor grid generation to identify the active sites surrounding the distance of 10X10X10 Å from the centroid of co-crystallized ligand (donepezil). The LigPrep module was used to generate the stable conformers of ligands (compound **6g** and donepezil), which were further docked using the Glide XP module of Schrödinger Maestro 2018–1. The detailed interaction analyses were performed using the Glide XP visualizer tool.

4.3.2. Molecular dynamics

Molecular dynamics simulation run of 20 nsec was performed to affirm the binding stability and pattern of compound **6g**-AChE complex using Desmond. Initially, the system was built using the system builder in which the virtual water environment was created by cubic simulation box of the TIP3P explicit water system with the minimum distance of 10 Å between the box wall and protein–ligand complex. The counterions were added to neutralize the system, and for the isosmotic salt environment, 0.15 M NaCl was added. Conjugate gradient algorithm with maximum 2000 interactions with convergence criteria of 1 kcal/mol/Å was used for the energy minimization of the system. After energy minimization, simulation run of 20 nsec was performed with periodic boundary condition under isothermal-isobaric ensemble (NPT), and the temperature and pressure of the system were set to 300 K and 1.013 atmospheric bar, respectively.

4.3.3. In silico estimation of drug-like properties

The drug-likeliness characteristics were predicted using the QikProp module of Schrödinger Maestro 2018–1. Several descriptors were predicted such as QPlogBB, log P, PSA (polar surface area) to determine the drug-likeliness property in the compound as per the Lipinski's rule of five (mol_MW < 500, QPlogPo/w < 5, donorHB ≤ 5, accptHB ≤ 10).

Conflicts of interest

Authors declare no conflict of interest.

Acknowledgments

The authors gratefully acknowledge the Central Instrument Facility (CIF), Indian Institute of Technology (Banaras Hindu University), Varanasi for conducting NMR experiments. We are also thankful to the Department of Health Research, Ministry of Health and Family Welfares for approving Young Scientist Grant to Mr. Piyoosh Sharma in newer areas of Drugs Chemistry (25011/215-HRD/2016-HR).

Appendix A. Supplementary material

Supplementary data to this article can be found online at https://doi.org/10.1016/j.bioorg.2018.12.017.

References

[1] A.A. Geronikaki, J.C. Dearden, D. Filimonov, I. Galaeva, T.L. Garibova, T. Gloriozova, V. Krajneva, A. Lagunin, F.Z. Macaev, G. Molodavkin, Design of new cognition enhancers: from computer prediction to synthesis and biological evaluation, J. Med. Chem. 47 (11) (2004) 2870–2876.
[2] R. Etcheberrigaray, D.L. Alkon, Methods for Alzheimer's Disease treatment and cognitive enhancement, in: E. Patent (Ed.) European Patent, Rockefeller Blanchette Neurosciences Institute 2004.
[3] Y. Xu, J. Yan, P. Zhou, J. Li, H. Gao, Y. Xia, Q. Wang, Neurotransmitter receptors and cognitive dysfunction in Alzheimer's disease and Parkinson's disease, Prog. Neurobiol. 97 (1) (2012) 1–13.
[4] M.-M. Mesulam, A. Guillozet, P. Shaw, A. Levey, E. Duysen, O. Lockridge, Acetylcholinesterase knockouts establish central cholinergic pathways and can use butyrylcholinesterase to hydrolyze acetylcholine, Neuroscience 110 (4) (2002) 627–639.
[5] A. Easton, V. Douchamps, M. Eacott, C. Lever, A specific role for septohippocampal acetylcholine in memory? Neuropsychologia 50 (13) (2012) 3156–3168.
[6] M. Zengin, H. Genc, P. Taslimi, A. Kestane, E. Guclu, A. Ogutlu, O. Karabay, İ. Gulçin, Novel thymol bearing oxypropanolamine derivatives as potent some metabolic enzyme inhibitors–Their antidiabetic, anticholinergic and antibacterial potentials, Bioorg. Chem. 81 (2018) 119–126.
[7] B. Yiğit, M. Yiğit, D. Barut Celepci, Y. Gök, A. Aktaş, M. Aygün, P. Taslimi, İ. Gülçin, Novel benzylic substituted imidazolinium, tetrahydropyrimidinium and tetrahydrodiazepinium salts: Potent carbonic anhydrase and acetylcholinesterase inhibitors, ChemistrySelect 3 (27) (2018) 7976–7982.
[8] P. Srivastava, P.N. Tripathi, P. Sharma, S.N. Rai, S.P. Singh, R.K. Srivastava, S. Shankar, S.K. Shrivastava, Design and development of some phenyl benzoxazole derivatives as a potent acetylcholinesterase inhibitor with antioxidant property to enhance learning and memory, Eur. J. Med. Chem. 163 (2018) 116–135.
[9] L. Peauger, R. Azzouz, V. Gembus, M.-L. Tintas, J. Sopková-de Oliveira Santos, P. Bohn, C. Papamicaël, V. Levacher, Donepezil-based central acetylcholinesterase inhibitors by means of a "bio-oxidizable" prodrug strategy: design, synthesis, and in vitro biological evaluation, J. Medi. Chem. 60 (13) (2017) 5909–5926.
[10] J. López-Arrieta, L. Schneider, Metrifonate for Alzheimer's disease, Cochrane database of systematic reviews (2) (2006).
[11] M. Mehta, A. Adem, M. Sabbagh, New acetylcholinesterase inhibitors for Alzheimer's disease, Int. J. Alzheimer's Disease 2012 (2012).
[12] R.K. Harrison, Phase II and phase III failures: 2013–2015, Nat. Rev. Drug Discovery 15 (12) (2016) 817–818.
[13] A. Kulshreshtha, P. Piplani, Ameliorative effects of amide derivatives of 1, 3, 4-thiadiazoles on scopolamine induced cognitive dysfunction, Eur. J. Med. Chem. 122 (2016) 557–573.
[14] C.P. LeBel, H. Ischiropoulos, S.C. Bondy, Evaluation of the probe 2', 7'-dichlorofluorescin as an indicator of reactive oxygen species formation and oxidative stress, Chem. Res. Toxicol. 5 (2) (1992) 227–231.
[15] I. Gülçin, Antioxidant activity of food constituents: an overview, Arch. Toxicol. 86 (3) (2012) 345–391.
[16] E. Bursal, E. Köksal, İ. Gülçin, G. Bilsel, A.C. Gören, Antioxidant activity and polyphenol content of cherry stem (Cerasus avium L.) determined by LC–MS/MS, Food Res. Int. 51 (1) (2013) 66–74.
[17] K. Jomova, D. Vondrakova, M. Lawson, M. Valko, Metals, oxidative stress and neurodegenerative disorders, Mol. Cell. Biochem. 345 (1–2) (2010) 91–104.
[18] B. Budzynska, A. Boguszewska-Czubara, M. Kruk-Slomka, K. Skalicka-Wozniak, A. Michalak, I. Musik, G. Biala, Effects of imperatorin on scopolamine-induced cognitive impairment and oxidative stress in mice, Psychopharmacology 232 (5) (2015) 931–942.
[19] G.A. Patani, E.J. LaVoie, Bioisosterism: a rational approach in drug design, Chem. Rev. 96 (8) (1996) 3147–3176.
[20] P. Singla, V. Luxami, K. Paul, Triazine as a promising scaffold for its versatile biological behavior, Eur. J. Med. Chem. 102 (2015) 39–57.
[21] M.G. Russell, R.W. Carling, L.J. Street, D.J. Hallett, S. Goodacre, E. Mezzogori, M. Reader, S.M. Cook, F.A. Bromidge, R. Newman, Discovery of imidazo [1, 2-b][1, 2, 4] triazines as GABAA α2/3 subtype selective agonists for the treatment of anxiety, J. Med. Chem. 49 (4) (2006) 1235–1238.
[22] H. Irannejad, H. Nadri, N. Naderi, S.N. Rezaeian, N. Zafari, A. Foroumadi, M. Amini, M. Khoobi, Anticonvulsant activity of 1, 2, 4-triazine derivatives with pyridyl side chain: synthesis, biological, and computational study, Med. Chem. Res. 24 (6) (2015) 2505–2513.
[23] M.J. Leach, C.M. Marden, A.A. Miller, Pharmacological studies on lamotrigine, a novel potential antiepileptic drug, Epilepsia 27 (5) (1986) 490–497.
[24] M. Congreve, S.P. Andrews, A.S. Doré, K. Hollenstein, E. Hurrell, C.J. Langmead, J.S. Mason, I.W. Ng, B. Tehan, A. Zhukov, Discovery of 1, 2, 4-triazine derivatives as adenosine A2A antagonists using structure based drug design, J. Med. Chem. 55 (5) (2012) 1898–1903.
[25] A.K. Sen Gupta, K. Hajela, T. Bhattacharya, S. Ahmad, K. Shanker, Synthesis and evaluation of AChE inhibitory activity of 5, 6-diaryl-1, 2, 4-triazinylox-yacetyl-4-substituted thiosemicarbazides, triazoles and N-benzylidene derivatives, Journal of Heterocyclic Chemistry 20(3) (1983) 507-510.
[26] Z. Jin, L. Yang, H. Xu, E. Huang, D.C. Wan, S. Li, H. Lin, C. Hu, Synthesis and biological activity of 3, 6-diaryl-7H-thiazolo [3, 2-b][1, 2, 4] triazin-7-one derivatives as novel acetylcholinesterase inhibitors, Sci. China Chem. 53 (11) (2010) 2297–2303.
[27] A. Sinha, R.S. Tamboli, B. Seth, A.M. Kanhed, S.K. Tiwari, S. Agarwal, S. Nair, R. Giridhar, R.K. Chaturvedi, M.R. Yadav, Neuroprotective role of novel triazine derivatives by activating Wnt/β catenin signaling pathway in rodent models of Alzheimer's disease, Mol. Neurobiol. 52 (1) (2015) 638–652.
[28] H. Irannejad, M. Amini, F. Khodagholi, N. Ansari, S.K. Tusi, M. Sharifzadeh, A. Shafiee, Synthesis and in vitro evaluation of novel 1, 2, 4-triazine derivatives as neuroprotective agents, Bioorg. Med. Chem. 18 (12) (2010) 4224–4230.
[29] E. Mezeiova, K. Spilovska, E. Nepovimova, L. Gorecki, O. Soukup, R. Dolezal, D. Malinak, J. Janockova, D. Jun, K. Kuca, Profiling donepezil template into multipotent hybrids with antioxidant properties, J. Enzyme Inhib. Med. Chem. 33 (1) (2018) 583–606.
[30] A.G. Banerjee, N. Das, S.A. Shengule, P.A. Sharma, R.S. Srivastava, S.K. Shrivastava, Design, synthesis, evaluation and molecular modelling studies of some novel 5, 6-diphenyl-1, 2, 4-triazin-3 (2H)-ones bearing five-member heterocyclic moieties as potential COX-2 inhibitors: A hybrid pharmacophore approach, Bioorg. Chem. 69 (2016) 102–120.
[31] A.G. Banerjee, N. Das, S.A. Shengule, R.S. Srivastava, S.K. Shrivastava, Synthesis, characterization, evaluation and molecular dynamics studies of 5, 6-diphenyl-1,2,4-triazin-3(2H)-one derivatives bearing 5-substituted 1,3,4-oxadiazole as potential anti-inflammatory and analgesic agents, Eur. J. Med. Chem. 101 (2015) 81–95.
[32] Ü.D. Özkay, Ö.D. Can, B.N. Sağlık, N. Turan, A benzothiazole/piperazine derivative with acetylcholinesterase inhibitory activity: Improvement in streptozotocin-induced cognitive deficits in rats, Pharmacol. Rep. 69 (6) (2017) 1349–1356.
[33] D. Panek, A. Więckowska, J. Jończyk, J. Godyń, M. Bajda, T. Wichur, A. Pasieka, D. Knez, A. Pišlar, J. Korabecny, Design synthesis and biological evaluation of 1-Benzylamino-2-hydroxyalkyl derivatives as new potential disease-modifying multifunctional anti-alzheimer's agents, ACS Chem. Neurosci. 9 (5) (2018) 1074–1094.
[34] J. Korabecny, K. Spilovska, E. Mezeiova, O. Benek, R. Juza, D. Kaping, O. Soukup, A systematic review on donepezil-based derivatives as potential cholinesterase inhibitors for Alzheimer's disease, Curr. Med. Chem. (2018).
[35] J. Korabecny, R. Dolezal, P. Cabelova, A. Horova, E. Hruba, J. Ricny, L. Sedlacek, E. Nepovimova, K. Spilovska, M. Andrs, 7-MEOTA–donepezil like compounds as cholinesterase inhibitors: synthesis, pharmacological evaluation, molecular modeling and QSAR studies, Eur. J. Med. Chem. 82 (2014) 426–438.
[36] J.M.M. Ezoulin, B.-Y. Shao, Z. Xia, Q. Xie, J. Li, Y.-Y. Cui, H. Wang, C.-Z. Dong, Y.-X. Zhao, F. Massicot, Novel piperazine derivative PMS1339 exhibits tri-functional properties and cognitive improvement in mice, Int. J. Neuropsychopharmacol. 12 (10) (2009) 1409–1419.
[37] N. Matsuoka, T.G. Aigner, FK960 [N-(4-acetyl-1-piperazinyl)-p-fluorobenzamide monohydrate], a novel potential antidementia drug, improves visual recognition memory in rhesus monkeys: comparison with physostigmine, J. Pharmacol. Exp. Ther. 280 (3) (1997) 1201–1209.
[38] A. Więckowska, T. Wichur, J. Godyń, A. Bucki, M. Marcinkowska, A. Siwek, K. Więckowski, P. Zaręba, D. Knez, M. Głuch-Lutwin, Novel multitarget-directed ligands aiming at symptoms and causes of alzheimer's disease, ACS Chem. Neurosci. (2018).
[39] L.B. Rubia, R. Gomez, TLC sensitivity of six modifications of Dragendorff's reagent, J. Pharm. Sci. 66 (11) (1977) 1656–1657.
[40] S.K. Shrivastava, P. Srivastava, R. Bandresh, P.N. Tripathi, A. Tripathi, Design, synthesis, and biological evaluation of some novel indolizine derivatives as dual cyclooxygenase and lipoxygenase inhibitor for anti-inflammatory activity, Bioorg Med. Chem. 25 (16) (2017) 4424–4432.
[41] A. Villalobos, J.F. Blake, C.K. Biggers, T.W. Butler, D.S. Chapin, Y.L. Chen, J.L. Ives, S.B. Jones, D.R. Liston, Novel benzisoxazole derivatives as potent and selective inhibitors of acetylcholinesterase, J. Med. Chem. 37 (17) (1994) 2721–2734.
[42] M. Recanatini, A. Cavalli, C. Hansch, A comparative QSAR analysis of acetylcholinesterase inhibitors currently studied for the treatment of Alzheimer's disease, Chem. Biol. Interact. 105 (3) (1997) 199–228.
[43] A. Rampa, A. Bisi, P. Valenti, M. Recanatini, A. Cavalli, V. Andrisano, V. Cavrini, L. Fin, A. Buriani, P. Giusti, Acetylcholinesterase Inhibitors: Synthesis and Structure− Activity Relationships of ω-[N-Methyl-N-(3-alkylcarbamoyloxyphenyl)-methyl] aminoalkoxyheteroaryl Derivatives, J. Med. Chem. 41 (21) (1998) 3976–3986.
[44] S.K. Shrivastava, P. Srivastava, T. Upendra, P.N. Tripathi, S.K. Sinha, Design, synthesis and evaluation of some N-methylenebenzenamine derivatives as selective

acetylcholinesterase (AChE) inhibitor and antioxidant to enhance learning and memory, Bioorg. Med. Chem. 25 (4) (2017) 1471–1480.
[45] W.K. Hagmann, The many roles for fluorine in medicinal chemistry, J. Med. Chem. 51 (15) (2008) 4359–4369.
[46] L. Piazzi, A. Cavalli, F. Belluti, A. Bisi, S. Gobbi, S. Rizzo, M. Bartolini, V. Andrisano, M. Recanatini, A. Rampa, Extensive SAR and computational studies of 3-{4-[(Benzylmethylamino) methyl] phenyl}-6, 7-dimethoxy-2 H-2-chromenone (AP2238) derivatives, J. Med. Chem. 50 (17) (2007) 4250–4254.
[47] M. Bajda, A. Więckowska, M. Hebda, N. Guzior, C.A. Sotriffer, B. Malawska, Structure-based search for new inhibitors of cholinesterases, Int. J. Mol. Sci. 14 (3) (2013) 5608–5632.
[48] P. Taylor, S. Lappi, Interaction of fluorescence probes with acetylcholinesterase Site and specificity of propidium binding, Biochemistry 14 (9) (1975) 1989–1997.
[49] L. Di, E.H. Kerns, K. Fan, O.J. McConnell, G.T. Carter, High throughput artificial membrane permeability assay for blood–brain barrier, Eur. J. Med. Chem. 38 (3) (2003) 223–232.
[50] A. Seth, P.A. Sharma, A. Tripathi, P.K. Choubey, P. Srivastava, P.N. Tripathi, S.K. Shrivastava, Design, synthesis, evaluation and molecular modeling studies of some novel N-substituted piperidine-3-carboxylic acid derivatives as potential anticonvulsants, Med. Chem. Res. 27 (4) (2018) 1206–1225.
[51] S.K. Shrivastava, B.K. Patel, P.N. Tripathi, P. Srivastava, P. Sharma, A. Tripathi, A. Seth, M.K. Tripathi, Synthesis, evaluation and docking studies of some 4-thiazolone derivatives as effective lipoxygenase inhibitors, Chem. Pap. (2018) 1–15.
[52] A. Wolf, B. Bauer, E.L. Abner, T. Ashkenazy-Frolinger, A.M. Hartz, A comprehensive behavioral test battery to assess learning and memory in 129S6/Tg2576 mice, PLoS ONE 11 (1) (2016) e0147733.
[53] A. Palmer, The activity of the pentose phosphate pathway is increased in response to oxidative stress in Alzheimer's disease, J. Neural Transm. 106 (3–4) (1999) 317–328.
[54] G.L. Ellman, K.D. Courtney, V. Andres Jr, R.M. Featherstone, A new and rapid colorimetric determination of acetylcholinesterase activity, Biochem. Pharmacol. 7 (2) (1961) 88–95.
[55] S.K. Shrivastava, S.K. Sinha, P. Srivastava, P.N. Tripathi, P. Sharma, M.K. Tripathi, A. Tripathi, P.K. Choubey, D.K. Waiker, L.M. Aggarwal, Design and development of novel p-aminobenzoic acid derivatives as potential cholinesterase inhibitors for the treatment of Alzheimer's disease, Bioorg. Chem. 82 (2019) 211–223.
[56] H. Lineweaver, D. Burk, The determination of enzyme dissociation constants, J. Am. Chem. Soc. 56 (3) (1934) 658–666.
[57] T. Mosmann, Rapid colorimetric assay for cellular growth and survival: application to proliferation and cytotoxicity assays, J. Immunol. Methods 65 (1–2) (1983) 55–63.
[58] Z. Bohdanecký, M. Jarvik, Impairment of one-trial passive avoidance learning in mice by scopolamine, scopolamine methylbromide, and physostigmine, Int. J. Neuropharmacol. 6 (3) (1967) 217–222.
[59] E.D. Wills, Mechanisms of lipid peroxide formation in animal tissues, Biochem. J. 99 (3) (1966) 667–676.
[60] D. Jollow, J. Mitchell, N.a. Zampaglione, J. Gillette, Bromobenzene-induced liver necrosis. Protective role of glutathione and evidence for 3, 4-bromobenzene oxide as the hepatotoxic metabolite, Pharmacology 11 (3) (1974) 151–169.
[61] Y. Kono, Generation of superoxide radical during autoxidation of hydroxylamine and an assay for superoxide dismutase, Arch. Biochem. Biophys. 186 (1) (1978) 189–195.
[62] L.C. Green, D.A. Wagner, J. Glogowski, P.L. Skipper, J.S. Wishnok, S.R. Tannenbaum, Analysis of nitrate, nitrite, and [15N] nitrate in biological fluids, Anal. Biochem. 126 (1) (1982) 131–138.
[63] G. Kryger, I. Silman, J.L. Sussman, Structure of acetylcholinesterase complexed with E2020 (Aricept®): implications for the design of new anti-Alzheimer drugs, Structure 7 (3) (1999) 297–307.